

Enhancement of superconductivity at the onset of charge-density-wave order in a metal

Yuxuan Wang¹ and Andrey V. Chubukov²

¹*Department of Physics, University of Wisconsin, Madison, WI 53706, USA*

²*William I. Fine Theoretical Physics Institute, and School of Physics and Astronomy, University of Minnesota, Minneapolis, MN 55455, USA*

(Dated: March 5, 2022)

We analyze superconductivity in the cuprates near the onset of an incommensurate charge density wave (CDW) order with momentum $\mathbf{Q} = (Q, 0)/(0, Q)$, as observed in the experiments. We first consider a semi-phenomenological charge-fermion model in which hot fermions, separated by \mathbf{Q} , attract each other by exchanging soft CDW fluctuations. We find that in a quantum-critical region near CDW transition, $T_c = A\bar{g}_c$, where \bar{g}_c is charge-fermion coupling and A is the prefactor which we explicitly compute. We then consider the particular microscopic scenario in which CDW order parameter emerges as a composite field made out of primary spin-density-wave fields. We show that charge-fermion coupling \bar{g}_c is of order of spin-fermion coupling \bar{g}_s . As the consequence, superconducting T_c is substantially enhanced near the onset of CDW order. Finally we analyze the effect of an external magnetic field H . We show that, as H increases, optimal T_c decreases and the superconducting dome becomes progressively more confined to the CDW quantum-critical point. These results are consistent with the experiments.

I. INTRODUCTION

Understanding of the nature of charge order in high- T_c cuprates and of its effect on superconductivity is essential for the full understanding of the complex physics in this materials. Charge order has been observed in the cuprates quite some time ago^{1,2}, but was originally thought to be present only in La-based materials. Recent wave of discoveries of an incommensurate charge-density-wave (CDW) order in Y-, Bi-, and Hg- based cuprates³⁻¹⁰ has demonstrated that charge order is ubiquitous to all families of high- T_c cuprates. A true long-range CDW order has so far been observed only in a finite magnetic field, but short-range static order (probably pinned by impurities) exists already in zero field. On a phase diagram, CDW order been detected within the pseudogap region, and its onset temperature is the highest around doping level $x \sim 0.12$. The CDW has an incommensurate momentum $\mathbf{Q} = Q_y = (0, Q)$ or $Q_x = (Q, 0)$ and the order is likely uni-axial, i.e., it develops, within a given domain, with only Q_x or Q_y (Ref. 8).

The discovery of the CDW order raised a number of questions about its origin¹¹⁻²¹, a potential discrete symmetry breaking before a true CDW order sets in^{4,14,22-28}, and the relation between CDW order (or its fluctuations) to pseudogap behavior^{14,18,20,27} and Fermi surface (FS) reconstruction²⁹.

In this paper we discuss another issue related to CDW – its effect on superconductivity. We take as inputs three experimental facts. First, T_c , as a function of doping, has a dip or a plateau at around $x \sim 0.12$, where the onset temperature of CDW is the largest^{30,31}. Second, when CDW is suppressed by applying pressure³², superconducting T_c increases. Third, when a magnetic field is applied³³, the dip grows and at high enough field the superconducting dome splits into two, and the one at larger

dopings is centered at the same x at which CDW order develops at $T = 0$ (Ref. 33). In other words, superconductivity forms a dome on top of quantum-critical point (QCP) for the onset of the CDW order.

The first two results can be naturally understood if we assume that CDW and d -wave superconductivity are just competing orders, i.e., when one order is at its peak, the other one is suppressed. The third observation, on the other hand, requires one to go beyond a simple “competing order” scenario because the presence of the dome of superconductivity on top of CDW QCP indicates that superconductivity is at least partly caused by soft fluctuations of CDW order which then must develop at larger energies than the ones related to superconductivity.

In our analysis we explore CDW-mediated superconductivity in some detail. We perform our analysis in two stages. At the first stage we put aside the issue what causes CDW order, assume that this order develops below some critical doping, and consider a semi-phenomenological model of fermions interacting by exchanging soft CDW fluctuations with momenta \mathbf{Q} . This model is quite similar to the spin-fermion model, considered in earlier studies of spin-mediated superconductivity for cuprates, Fe-pnictides, and other correlated materials³⁴⁻³⁹, and we dub this model the “charge-fermion model”. The charge-fermion and spin-fermion models are similar but differ in detail because of the difference between the CDW momentum \mathbf{Q} and antiferromagnetic momentum (π, π) , and also because of the difference in the spin structures of charge-mediated and spin-mediated interactions (spin Kronecker δ functions vs spin Pauli matrices). One qualitative consequence of these differences is that charge-mediated interaction gives rise to superconductivity with a full gap in each region where the FS crosses the Brillouin zone boundary (anti-nodal regions in the cuprate terminology), but it does not couple superconducting order parameters from different regions,

hence it alone cannot distinguish between s -wave and d -wave pairing symmetries⁴⁰.

We perform quantitative analysis of the pairing within the charge-fermion model in the most interesting quantum-critical regime right above QCP for CDW order. In this regime, charge-mediated interaction gives rise to the pairing but also destroys coherence of hot fermions (the ones at the FS separated by \mathbf{Q}). Superconducting T_c^{ch} is determined by the interplay between strong tendency towards pairing and strong pair-breaking effects associated with the self-energy. We compute Landau damping of soft bosons and fermionic self-energy, and then obtain and solve the linearized gap equation with renormalized fermionic and bosonic propagators. We show that in the quantum-critical region T_c is finite and scales with the effective charge-fermion coupling constant \bar{g}_c : $T_c^{\text{ch}} = A_c \bar{g}_c$, where $A_c \approx 0.0025$.

At the second stage we consider the specific microscopic scenario for CDW order – the one in which CDW is a composite order parameter made out of primary (π, π) spin fluctuations. Within this scenario, spin fluctuations are assumed to develop first, at energies comparable to bandwidth, while CDW fluctuations develop at smaller energies and do not provide substantial feedback on spin fluctuations. This composite order scenario requires fermion-fermion interaction to be comparable to the bandwidth (otherwise spin fluctuations do not develop at high energies) and inevitably is partly phenomenological. We will not discuss a complementary, renormalization group-based, truly weak coupling scenario in which all fluctuations (spin, charge, superconducting) develop simultaneously at low energy and mutually affect each other⁴¹.

Various versions of magnetically induced charge bond and site orders have been proposed over the last few years^{11–14,16–18,20,21,42,43}, some focused on CDW with diagonal momentum (Q, Q) , and others on CDW with momenta $Q_x = (Q, 0)$ and $Q_y = (0, Q)$. Motivated by experiments, we base our discussion on the soft fluctuations of axial CDW with momenta Q_x or Q_y . Previous studies have found⁴⁴ that axial CDW has a partner – an incommensurate pair-density wave (PDW), and fluctuations in CDW and PDW channels develop simultaneously. To keep presentation focused, we concentrate on CDW and neglect PDW fluctuations. The latter can in principle also mediate pairing interaction, but are unlikely to destructively interfere with CDW fluctuations.

In an earlier work¹⁴ we have shown that the axial CDW order develops in a paramagnet at a finite T_{cdw} , provided that magnetic correlation length ξ_s is large enough. As ξ_s decreases, T_{cdw} also decreases and vanishes at some finite $\xi_{s,\text{cr}}$, setting up a CDW QCP at a finite distance from a magnetic QCP (the one at $\xi_s = \infty$). Near $\xi_{s,\text{cr}}$ CDW fluctuations become soft and give rise to singular pairing interaction mediated by these fluctuations. We show the behavior of T_{cdw} vs ξ_s schematically in Fig. 1.

Whether this additional pairing interaction substantially affects superconducting T_c depends on the inter-

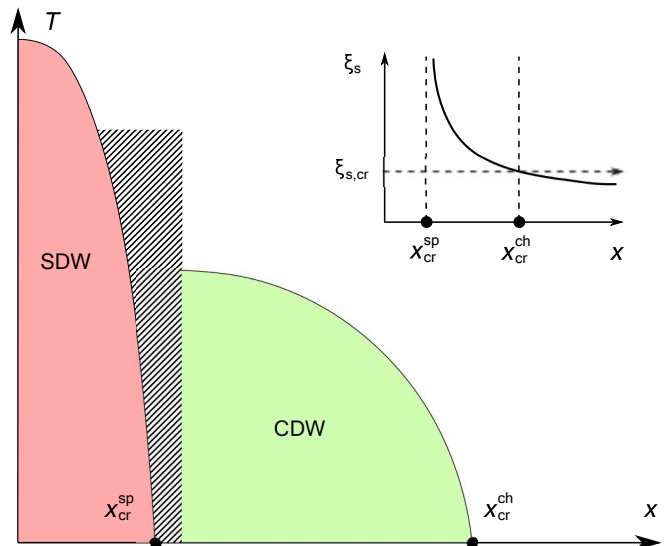


FIG. 1. Doping range where CDW order with momentum $(Q, 0)$ or $(0, Q)$ emerges within itinerant spin-fluctuation scenario. The effective interaction in the CDW channel is made out of two spin-fluctuation propagators. The CDW order develops only when the system is sufficiently close to a magnetic instability and terminates at doping $x_{\text{cr}}^{\text{ch}}$, different from $x_{\text{cr}}^{\text{sp}}$ for antiferromagnetism. In the shaded region near $x_{\text{cr}}^{\text{sp}}$ localization of electronic states (Mott physics) becomes relevant (Ref. 45), and spin-fluctuation approach needs to be modified. In this region, the onset temperature of CDW order drops.

play between charge-fermion coupling \bar{g}_c and the coupling \bar{g}_s between fermions and primary spin fluctuations. The argument is that spin-fluctuation exchange by itself gives rise to superconducting pairing, and at large ξ_s the corresponding T_c^{sp} scales with \bar{g}_s : $T_c^{\text{sp}} = A_s \bar{g}_s$, where $A_s \approx 0.007$ (Ref. 46). As ξ_s decreases, T_c^{sp} also decreases but remains finite. The two-dome structure of $T_c(x)$, observed in the cuprates in an applied magnetic field, can be understood within this approach only if near $\xi_s = \xi_{s,\text{cr}}$, $T_c^{\text{ch}} \geq T_c^{\text{sp}}$. If this does not hold, i.e., T_c^{ch} is smaller than T_c^{sp} , the contribution to superconductivity from charge-mediated exchange is only subdominant to the one from spin fluctuations. In this situation, the only effect on T_c from CDW is due to direct competition between CDW and superconducting orders. This competition may give rise to additional reduction of T_c in a magnetic field, given the experimental evidence that CDW order increases in a field. However, it cannot give rise to a peak of T_c above CDW QCP.

We evaluate charge-fermion coupling \bar{g}_c within the RPA-type analysis of charge fluctuations near CDW QCP: $U_c^{\text{eff}}(q) \propto U_c / (1 - U_c \Pi_c(q)) \equiv \bar{g}_c / (\xi_c^{-2} + (q - Q)^2)$, and show that \bar{g}_c is comparable to spin-fermion coupling \bar{g}_s . This result may look strange because charge fluctuations, viewed as composite objects made out of spin fluctuations, develop only in a narrow range near the FS points separated by Q_x or Q_y , with the width in momentum space of order $\Lambda \sim \xi_s^{-1}$. As the consequence,

$\bar{g}_c \sim U_c \xi_s^{-2}$. However, the “bare” interaction in the charge channel, U_c , is a composite object made out of two spin fluctuation propagators and two fermionic Green’s functions (see Fig. 8). This composite object behaves as $\bar{g}_s \xi_s^2$. As the consequence, $U_c \xi_s^{-2}$ is not reduced by ξ_s , and \bar{g}_c differs from \bar{g}_s only by a numerical factor.

To properly calculate the ratio \bar{g}_c/\bar{g}_s one needs to do full-scale dynamical calculations, even if one restricts with ladder series of diagrams, like in RPA. In this work, we use a simplification and approximate the bare interaction in the charge channel U_c by a constant within the momentum range $\Lambda \sim \xi_s^{-1}$ around proper Fermi surface points (hot spots) and set it to zero outside this range. We compute the polarization operator $\Pi_c(q, \Omega_m)$ and use RPA to obtain charge-mediated effective interaction within fermions. We use the condition for CDW QCP: $1 = U_c \Pi_c(Q)$ to fix Λ and obtain explicit relation between \bar{g}_c and \bar{g}_s . Within this approach, we find $\bar{g}_c \geq \bar{g}_s$.

We argue, based on this analysis, that the enhancement of superconductivity near a CDW QCP is substantial, i.e superconductivity in the cuprates comes from both spin and charge fluctuations. We present the schematic phase diagram in Fig. 2. This scenario explains the developments of two domes of T_c in a high magnetic field: one, at smaller doping, is due to critical spin fluctuations, and another, at larger doping, is due to critical charge fluctuations.

1. Relation to earlier works

The pairing by charge fluctuations has been studied before. In the context of the cuprates, DiCastro, Castellani, Grilli, and their collaborators⁴⁰ analyzed in detail the pairing mediated by axial CDW fluctuations near the onset of charge order, which was assumed to develop on its own rather than being induced by SDW fluctuations. They found that charge-mediated 4-fermion interaction is attractive in both d -wave and s -wave channel and does not distinguish the two. They argued that some other mechanism, e.g., antiferromagnetic spin fluctuations, lifts the degeneracy in favor of d -wave. We obtain the same results in Sec. II. The novel part of our analysis in this Section is the calculation of charge-mediated T_c in the quantum-critical regime.

This pairing problem near CDW QCP has certain similarities to the pairing at the onset of a nematic order, which has been extensively studied in recent years^{47–50}. It has been argued that $\mathbf{Q} = 0$ nematic fluctuations enhance all partial components of the pairing susceptibility. The case of QCP at small Q_x/Q_y is less unrestrictive in this respect but still, s -wave and d -wave channels are degenerate for CDW fluctuations.

The analysis of the electron-mediated pairing near a QCP for density-wave order is also quite interesting from a general perspective as it adds one important new element not present for the pairing away from a QCP.

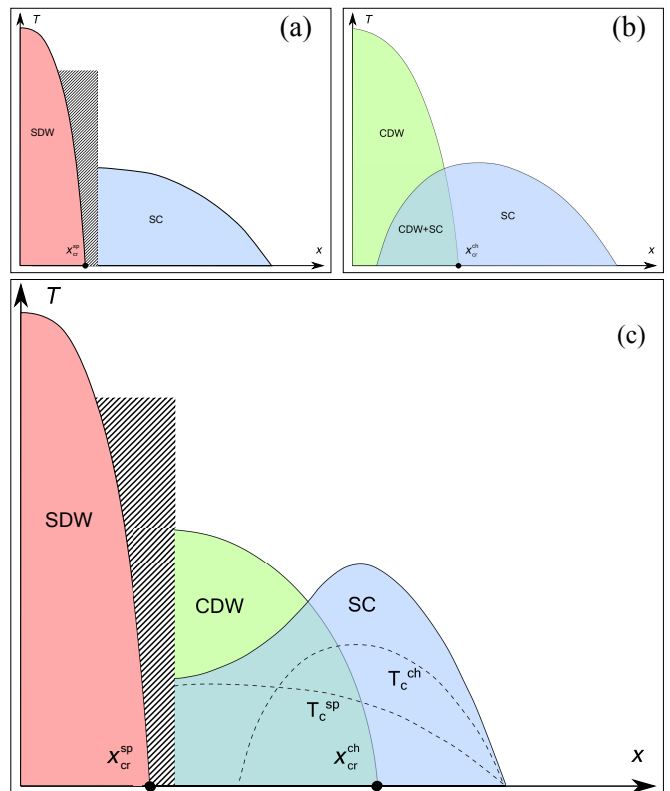


FIG. 2. Schematic phase diagram for the interplay between superconductivity mediated by spin and charge fluctuations. Panel (a): the onset temperature T_c^{sp} of spin-mediated superconductivity, as a function of doping. We assume that impurities kill superconductivity above a certain doping. Panel (b): the onset temperature T_c^{sp} of charge-mediated superconductivity near the onset of CDW order. We compute T_c^{ch} in this work. Panel (c): The full phase diagram. The non-monotonic $T_c(x)$ is obtained by combining spin-mediated and charge-mediated contributions to T_c from panels (a) and (b) (dashed lines).

Namely, the same interaction which gives rise to strong attraction also destroys fermionic coherence and prevent fermions from developing supercurrent^{51,52}. Superconductivity then may or may not emerge depending on the interplay between these two opposite tendencies^{47,53}.

The rest of this paper is organized as follows. In Sec. II we introduce and analyze charge-fermion model of itinerant electrons coupled to near-critical CDW fluctuations. In Sec. IIa we derive bosonic and fermionic self-energies. In Sec. IIb we study the pairing problem and obtain T_c^{ch} due to charge-fluctuation exchange near a CDW QCP. We show that T_c^{ch} scales with the charge-fermion coupling constant \bar{g}_c . In Sec. III, we relate \bar{g}_c and spin-fermion coupling \bar{g}_s within the magnetic scenario for CDW. In this scenario, a CDW order parameter field emerges as a composite object made out of two spin-fluctuation propagators. We show that \bar{g}_c is comparable to \bar{g}_s and may even exceed it. In Sec. IV we discuss in some more detail superconducting dome around CDW QCP. Finally in

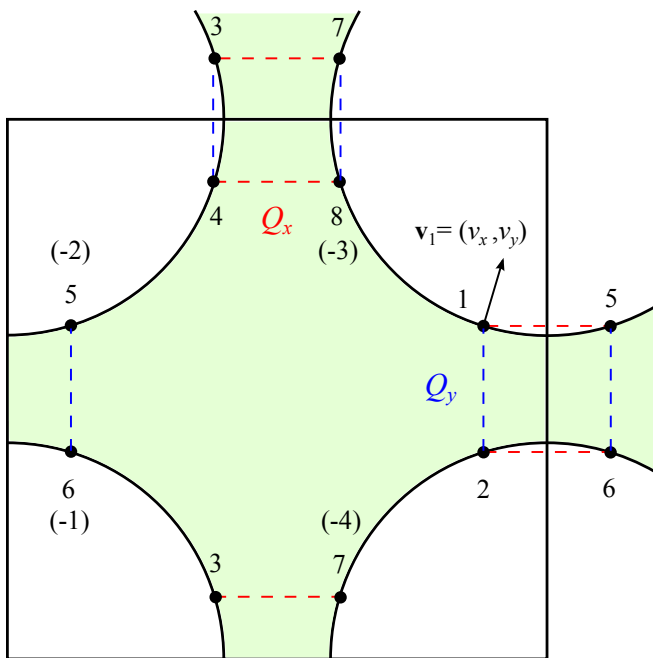


FIG. 3. The Fermi surface of a 2D electronic system on a square lattice and location of hot spots for charge-mediated interaction. CDW “hot” spots are defined as points on the Fermi surface separated by either $Q_y = (0, Q)$ or by $Q_x = (Q, 0)$. In a generic situation, there are 8 hot spots for Q_y and eight for Q_x . Motivated by experiments, we consider the case when hot spots for Q_y and for Q_x merge. In this situation, CDW hot spots coincide with hot spots for (π, π) magnetism, and there are eight of them on the Fermi surface. We label these hot spots by 1-8 ($5 \equiv -2$, $6 \equiv -1$, etc.). The arrow shows the direction of the Fermi velocity at hot spot 1. Fermi velocities at other seven hot spots are related to this one by symmetry. Near CDW instability hot fermions interact with each other by exchanging CDW fluctuations with momenta $Q_{x,y}$. Here and in other figures below we represent charge fluctuations by dashed lines.

Sec. V we discuss the results and present our conclusions.

II. THE CHARGE-FERMION MODEL

We begin with a semi-phenomenological analysis. We assume, without specifying the reason, that CDW order with momentum $Q_y = (0, Q)$ and/or $Q_x = (Q, 0)$, develops at some critical doping x_c^{cr} , and consider the model of 2D fermions interacting by exchanging near-critical, soft charge fluctuations. We dub this model as “charge-fermion model” by analogy with the spin-fermion model which was introduced to describe a system near a magnetic QCP. As our goal is to describe low-energy physics (energies well below the bandwidth), we focus on momentum ranges around the CDW “hot” spots on the FS, defined as points which are separated by CDW momentum Q_x or Q_y . For a generic \mathbf{Q} there are 16 CDW hot spots, eight corresponding to Q_y and another eight cor-

responding to Q_x . For simplicity we consider the case when \mathbf{Q} is such that CDW hot spots are at or near the crossing between the FS and symmetry lines in the Brillouin zone $k_x \pm k_y = \pm\pi$. Then hot spots from Q_y sector merge with hot spots from Q_x sector, and the total number of hot spots become eight. We label these points as 1-8 in Fig. 3. This approximation works reasonably well for the values of \mathbf{Q} extracted from the experiments⁶.

We linearize the fermionic dispersion in the vicinity of a hot spot i as $\epsilon_{i,\tilde{\mathbf{k}}} = \mathbf{v}_i \cdot \tilde{\mathbf{k}}_i$, where \mathbf{v}_i is the Fermi velocity and $\tilde{\mathbf{k}}_i$ is the momentum deviation from the hot spot i . We define the Fermi velocity at the hot spot 1 as $\mathbf{v}_1 = (v_x, v_y)$, the velocities at other hot spots are related by symmetry. In the cuprates, the FS at the antinodal region is “flattened”, and we have $v_x < v_y$ (see Fig. 3). We define $\alpha = v_x/v_y < 1$.

The action of the charge-fermion model can be written as

$$\begin{aligned} \mathcal{S} = & \int d\tilde{\mathbf{k}} \sum_{i,\alpha} c_{i\alpha}^\dagger(\tilde{\mathbf{k}}) (-i\omega_m + \epsilon_{i\tilde{\mathbf{k}}}) c_{i,\alpha}(\tilde{\mathbf{k}}) \\ & + \int d\tilde{\mathbf{q}} \chi_{0c}^{-1}(\tilde{\mathbf{q}}) \sum_{a=x,y} \phi_a(\tilde{\mathbf{q}}) \phi_a^\dagger(\tilde{\mathbf{q}}) \\ & + g_c \sum_{\alpha} f_y^i \int d\tilde{\mathbf{k}} d\tilde{\mathbf{k}}' c_{i\alpha}^\dagger(\tilde{\mathbf{k}}) c_{i+1,\alpha}(\tilde{\mathbf{k}}') \phi_y^\dagger(\tilde{\mathbf{k}} - \tilde{\mathbf{k}}') \\ & + g_c \sum_{\alpha} f_x^i \int d\tilde{\mathbf{k}} d\tilde{\mathbf{k}}' c_{i\alpha}^\dagger(\tilde{\mathbf{k}}) c_{i+4,\alpha}(\tilde{\mathbf{k}}') \phi_x^\dagger(\tilde{\mathbf{k}} - \tilde{\mathbf{k}}') \\ & + h.c., \end{aligned} \quad (1)$$

where $c_{i\alpha}$ is a fermion field with i labeling hot spots and α labeling spin projections. Hot spots i and $i+1$ are separated by CDW momentum Q_y , and hot spots i and $i+4$ are separated by Q_x (see Fig. 3). The scalar field $\phi_{x,y}$ is a CDW order parameter field with momenta near Q_x/Q_y . In Eq. (1) we have used short-hands $\tilde{\mathbf{k}} = (\omega_m, \tilde{\mathbf{k}})$ and $\tilde{\mathbf{q}} = (\Omega_m, \tilde{\mathbf{q}})$, where ω_m (Ω_m) are fermionic (bosonic) Matsubara frequencies. The bosonic momentum $\tilde{\mathbf{q}}$ is measured as the deviation from CDW momenta Q_x or Q_y , and the fermionic momentum $\tilde{\mathbf{k}}$ is measured as the deviation from the corresponding hot spot. The form-factors $f_{x,y}^i$ determine relative magnitude and sign between CDW orders in different hot regions. In general, the CDW order has both d -wave and s -wave components. A pure d -wave order would correspond to $f_y^{1,5} = -f_y^{3,7} = 1$ and $f_x^{1,2} = -f_x^{3,4} = 1$.

We assume, like it is done in the spin-fermion model, that static charge susceptibility comes from fermions with energies larger than the one relevant to superconductivity and approximate it by a simple Ornstein-Zernike form $\chi_c = \chi_{0c}/(\tilde{q}_x^2 + \tilde{q}_y^2 + \xi_c^{-2})$, where ξ_c is the CDW correlation length. The prefactors for \tilde{q}_x^2 and \tilde{q}_y^2 may in general differ⁵⁴ because Q_x and Q_y are not along Brillouin zone diagonals, but this difference can be absorbed into rescaling of $\tilde{\mathbf{q}}$ and does not affect our analysis.

The coupling g_c is a phenomenological charge-fermion coupling constant. The corresponding charge-mediated 4-fermion interaction term in the Hamiltonian is (we set $\mathbf{Q} = Q_y$ for definiteness)

$$\mathcal{H}_{\text{int}} = -U_c^{\text{eff}}(\mathbf{q}) \sum_{k,p} c_{k,\alpha}^\dagger c_{p,\gamma}^\dagger c_{k-q,\delta} c_{k+q,\beta} \delta_{\alpha\beta} \delta_{\gamma\delta} \quad (2)$$

with

$$U_c^{\text{eff}}(\mathbf{q}) = g_c^2 \chi_c(\mathbf{q}) = \frac{\bar{g}_c}{\xi_c^{-2} + (\mathbf{q} - \mathbf{Q}_y)^2}. \quad (3)$$

The effective coupling $\bar{g}_c = g_c^2 \chi_{0c}$, and the sign convention is such that the interaction appears with a factor -1 in the diagrammatic theory.

The charge-fermion model is defined self-consistently when its fluctuations cannot modify the physics at lattice energies, and this requires that \bar{g}_c must be small compared to the fermionic bandwidth.

A. Normal state analysis

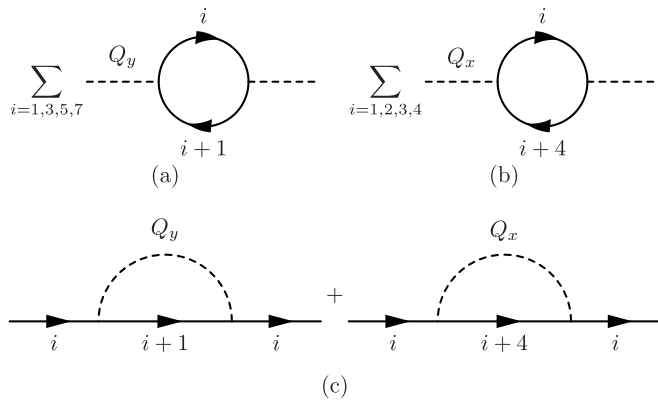


FIG. 4. The one-loop diagrams for the bosonic self-energy $\Pi_{x,y}$ [Panels (a), (b)] and fermionic self-energy Σ_i [Panel (c)].

For the computation of superconducting T_c^{ch} , mediated by charge fluctuations, we need to know normal state properties. We use Eq. (1) and compute self-energies for the bosonic fields ϕ_x and ϕ_y and for the fermionic field. We show corresponding diagrams in Fig. 4. We compute bosonic and fermionic self-energies in a self-consistent fashion, like it was done in the earlier works on the spin-fermion model^{11,52,55}. Namely, we first evaluate one-loop bosonic self-energy (the bosonic polarization operator) using free fermions and show that it has

the form of Landau damping, then use the full dynamical bosonic propagator to calculate one-loop fermionic self-energy and show that it is strong but predominantly depends on frequency, and then verify that frequency dependent fermionic self-energy does not affect the Landau damping. This self-consistent procedure becomes exact if we neglect subleading terms in the self-energy, which depend on the fermionic dispersion ϵ_k . This can be rigorously justified if we extend the model to M fermionic flavors and take the limit $M \rightarrow \infty$ (e.g. Ref. 11), or extend the number of pairs of hot spots from 4 to N and take the limit $N \rightarrow \infty$ (e.g. Ref. 52). We will use the latter extension to justify our analysis.

1. bosonic polarization operators

The bosonic polarization operator for ϕ_y is given by the diagram in Fig. 4(a), and the expression for ϕ_x is related by symmetry. The full polarization operator is a sum of contributions from four pairs of hot fermions which are separated by Q_y . These pairs are (1,2), (3,4), (5,6), and (7,8). There are no Umklapp processes for incommensurate CDW order, in distinction to SDW case in which $\mathbf{Q} = (\pi, \pi)$ and Umklapp processes are allowed.

For the contribution to Π from fermion pair (1,2) we obtain

$$\Pi_1(\Omega_m, \tilde{\mathbf{q}}) = -2g_c^2 T \sum_{\omega_m, \tilde{\mathbf{k}}} G_1(\omega_m, \tilde{\mathbf{k}}) G_2(\omega_m + \Omega_m, \tilde{\mathbf{k}} + \tilde{\mathbf{q}}) \quad (4)$$

where the factor 2 comes from summation over spin indices. To simplify the notations we will drop the tildes on momenta hereafter. The Green's functions are given by $G_{1,2} = 1/(i\omega_m - \epsilon_{1,2})$ and fermionic dispersions can be written as $\epsilon_{1,2} = \mathbf{v}_{1,2} \cdot \mathbf{k}$. We transform the momentum integral $dk_x dk_y$ into $d\epsilon_1 d\epsilon_2$ by adding the Jacobian $J = 1/|\mathbf{v}_1 \times \mathbf{v}_2| = 1/v_F^2 \times (\alpha^2 + 1)/(2\alpha)$, where $v_F = \sqrt{v_x^2 + v_y^2}$. Because this Jacobian is independent of \mathbf{q} , the polarization operator in this approximation is a function of frequency only. We subtract from $\Pi_1(\Omega_m)$ its frequency-independent part $\Pi_1(0)$, which only renormalizes the position of the CDW QCP and is not of interest to us. The subtraction makes integral over internal frequency convergent, and evaluating the integrals we obtain at zero temperature

$$\begin{aligned}
\Pi_1(\Omega_m) &= -\frac{g_c^2}{4\pi^3 v_F^2} \frac{\alpha^2 + 1}{\alpha} \int d\omega_m d\epsilon_1 d\epsilon_2 \left[\frac{1}{(i\omega_m - \epsilon_1)[i(\omega_m + \Omega_m) - \epsilon_2]} - \frac{1}{(i\omega_m - \epsilon_1)(i\omega_m - \epsilon_2)} \right] \\
&= \frac{g_c^2}{4\pi v_F^2} \frac{\alpha^2 + 1}{\alpha} \int d\omega_m [\text{sgn}(\omega_m) \text{sgn}(\omega_m + \Omega_m) - 1] \\
&= -\frac{g_c^2}{4\pi v_F^2} \frac{\alpha^2 + 1}{\alpha} |\Omega_m|. \tag{5}
\end{aligned}$$

This is a conventional Landau damping term. We do the same calculation for hot spot pairs (3,4), (5,6), and (7,8). Because the Jacobians $1/|\mathbf{v}_1 \times \mathbf{v}_2| = 1/|\mathbf{v}_3 \times \mathbf{v}_4| = 1/|\mathbf{v}_5 \times \mathbf{v}_6| = 1/|\mathbf{v}_7 \times \mathbf{v}_8| = 1/v_F^2 \times (\alpha^2 + 1)/(2\alpha)$, all contributions are the same as (5). Therefore $\Pi_y(\Omega_m) = 4\Pi_1(\Omega_m)$. It is easy to verify that for ϕ_x the self-energy is the same as for ϕ_y , i.e., $\Pi_x = \Pi_y$.

Including the polarization operator into the propagators for ϕ_x and ϕ_y fields, we obtain

$$\chi_c(\Omega_m, \mathbf{q}) = \frac{\chi_{0c}}{\xi_c^{-2} + q_x^2 + q_y^2 + \gamma_c |\Omega_m|}, \tag{6}$$

where

$$\gamma_c = \frac{4\bar{g}_c}{4\pi v_F^2} \frac{\alpha^2 + 1}{\alpha} \tag{7}$$

and we recall that $\bar{g}_c = g_c^2 \chi_{0c}$. The overall factor of 4 in the numerator of (7) is the number of pairs of hot fermions. To extend the model to large N one just has to replace 4 by N . We will use this extension below.

The total dynamical interaction mediated by charge fluctuations can then be written as

$$U_c^{\text{eff}}(\mathbf{q}, \Omega_m) = g_c^2 \chi(\mathbf{q}) = \frac{\bar{g}_c}{\xi_c^{-2} + (\mathbf{q} - \mathbf{Q}_x)^2 + \gamma_c |\Omega_m|}. \tag{8}$$

2. fermionic self-energy

We now use Eq. (6) and evaluate one-loop fermionic self-energy. The corresponding diagram is presented in Fig. 4(c). Observe that for any hot fermion, interactions mediated by both bosonic fields, ϕ_x and ϕ_y , contribute to the self-energy. For example, for a fermion at hot spot 1, ϕ_x and ϕ_y scatter it to hot spots 2 and 5, respectively.

The self-energy depends on the location of a fermion on the FS and on the distance to CDW QCP. Below we will be interested in superconductivity right at CDW QCP, hence we will need the self-energy right at this point. Accordingly, we set $\xi_c^{-1} = 0$ in the charge fluctuation propagator.

For the self-energy contribution to a fermion at hot

spot 1 from Q_y scattering, we have

$$\Sigma_y(\mathbf{k}, \omega_m) = T \sum_{\omega'_m, \mathbf{k}'} U_c^{\text{eff}}(\mathbf{k} - \mathbf{k}', \omega_m - \omega'_m) G_2(\omega'_m, \mathbf{k}'), \tag{9}$$

where \mathbf{k} is the deviation from hot spot 1. We place \mathbf{k} on the FS, i.e., set $k_{\perp} \equiv \hat{\mathbf{v}}_1 \cdot \mathbf{k} = 0$, which gives $k_y = -\alpha k_x$. At $T = 0$, we rewrite Eq. (9) as

$$\begin{aligned}
\Sigma_y(k_{\parallel}, \omega_m) &= \frac{-\bar{g}_c}{8\pi^3} \int \frac{d\omega'_m dk'_{\perp} dk'_{\parallel}}{i\omega'_m - v_F k'_{\perp}} \\
&\times \frac{1}{(\bar{k}_{\parallel} - k'_{\parallel})^2 + (\bar{k}_{\perp} - k'_{\perp})^2 + \gamma_c |\omega_m - \omega'_m|}, \tag{10}
\end{aligned}$$

where k'_{\perp} and k'_{\parallel} are perpendicular and parallel components of \mathbf{k}' with respect to the Fermi surface at hot spot 2, i.e., $k'_{\perp} \equiv \hat{\mathbf{v}}_2 \cdot \mathbf{k}'$, and \bar{k}_{\parallel} and \bar{k}_{\perp} are components of external \mathbf{k} , defined relative to the FS at the hot spot 2, i.e., $\bar{k}_{\perp} \equiv \hat{\mathbf{v}}_2 \cdot \mathbf{k}$, where $\mathbf{v}_2 = (v_x, -v_y)$. Using $k_y = -\alpha k_x$ we obtain

$$\bar{k}_{\perp} = 2\alpha k_{\parallel} / (\alpha^2 + 1). \tag{11}$$

We integrate over k'_{\perp} first, and complete the integration contour over the half plane with only one pole. We obtain

$$\begin{aligned}
\Sigma_y(k_{\parallel}, \omega_m) &= \frac{i\bar{g}_c}{8\pi^2 v_F} \int \frac{dk'_{\parallel} d\omega'_m \text{sgn}(\omega'_m)}{\sqrt{(\bar{k}_{\parallel} - k'_{\parallel})^2 + \gamma_c |\omega_m - \omega'_m|}} \\
&\frac{1}{\sqrt{(\bar{k}_{\parallel} - k'_{\parallel})^2 + \gamma_c |\omega_m - \omega'_m|} + [|\omega'_m|/v_F + i\bar{k}_{\perp} \text{sgn}(\omega'_m)]} \tag{12}
\end{aligned}$$

We will see that typical internal frequencies ω'_m are of the same order as external ω_m . Then, at small enough frequencies one can safely neglect the $|\omega'_m|/v_F$ term in the denominator. With this simplification we obtain

$$\begin{aligned}
\Sigma_y(k_{\parallel}, \omega_m) &= \frac{i\bar{g}_c}{8\pi^2 v_F} \int \frac{dk'_{\parallel} d\omega'_m \text{sgn}(\omega'_m)}{(\bar{k}_{\parallel} - k'_{\parallel})^2 + \gamma_c |\omega_m - \omega'_m| + \bar{k}_{\perp}^2} \\
&= \frac{i\bar{g}_c}{2\pi v_F \gamma_c} \text{sgn}(\omega_m) \left[\sqrt{\gamma_c |\omega_m| + \bar{k}_{\perp}^2} - |\bar{k}_{\perp}| \right]. \tag{13}
\end{aligned}$$

Plugging Eq. (11) into Eq. (13) we finally obtain

$$\begin{aligned}\Sigma_y(k_{\parallel}, \omega_m) &= \frac{i\bar{g}_c}{2\pi v_F \gamma_c} \text{sgn}(\omega_m) \\ &\times \left[\sqrt{\gamma_c |\omega_m| + \left(\frac{2\alpha k_{\parallel}}{\alpha^2 + 1}\right)^2} - \left| \frac{2\alpha k_{\parallel}}{\alpha^2 + 1} \right| \right] \\ &= \frac{2iv_F}{N} \frac{\alpha}{\alpha^2 + 1} \text{sgn}(\omega_m) \\ &\times \left[\sqrt{\gamma_c |\omega_m| + \left(\frac{2\alpha k_{\parallel}}{\alpha^2 + 1}\right)^2} - \left| \frac{2\alpha k_{\parallel}}{\alpha^2 + 1} \right| \right].\end{aligned}\quad (14)$$

The self-energy from Q_x scattering is obtained in the same way:

$$\Sigma_x(\mathbf{k}, \omega_m) = -\bar{g}_c T \sum_{\omega'_m, \mathbf{k}'} \chi_c(\omega_m - \omega'_m, \mathbf{k} - \mathbf{k}') G_5(\omega'_m, \mathbf{k}'). \quad (15)$$

As Fermi velocities at hot spot 5 and 2 are antiparallel, we have $G_5(\omega'_m, \mathbf{k}') = G_2(\omega'_m, -\mathbf{k}')$. Comparing Eqs. (9) and (15), we then immediately find that $\Sigma_x = \Sigma_y$. Combining the two we obtain

$$\begin{aligned}\Sigma(k_{\parallel}, \omega_m) &= \frac{i\bar{g}_c}{\pi v_F \gamma_c} \text{sgn}(\omega_m) \\ &\times \left[\sqrt{\gamma_c |\omega_m| + \left(\frac{2\alpha k_{\parallel}}{\alpha^2 + 1}\right)^2} - \left| \frac{2\alpha k_{\parallel}}{\alpha^2 + 1} \right| \right] \\ &= \frac{4iv_F}{N} \frac{\alpha}{\alpha^2 + 1} \text{sgn}(\omega_m) \\ &\times \left[\sqrt{\gamma_c |\omega_m| + \left(\frac{2\alpha k_{\parallel}}{\alpha^2 + 1}\right)^2} - \left| \frac{2\alpha k_{\parallel}}{\alpha^2 + 1} \right| \right].\end{aligned}\quad (16)$$

It is easy to verify that this results holds for around all hot regions 1-8, and in each region k_{\parallel} is the deviation from the corresponding hot spot along the FS. The functional form of the self-energy as in Eq. (16) was first obtained for the spin-fermion model in Ref. 52 (for $\alpha = 1$) and Ref. 11 (for arbitrary α). Right at a hot spot, the fermionic self-energy has a non-Fermi liquid (NFL) form:

$$\Sigma(0, \omega_m) = i \text{sgn}(\omega_m) \sqrt{\omega_{0c} |\omega_m|}, \quad (17)$$

where $\omega_{0c} = (4/N)\bar{g}_c/\pi \times \alpha/(\alpha^2 + 1)$. Away from a hot spot, at $k_{\parallel}^2 \gg \gamma_c |\omega_m|$, the self-energy $\Sigma(\omega_m, k_{\parallel})$ retains a Fermi liquid (FL) form at the smallest ω_m , i.e., we have

$$\Sigma(\omega_m, k_{\parallel}) = \frac{i\omega_m}{|k_{\parallel}|} \left(\frac{\bar{g}_c}{\pi v_F} \frac{\alpha^2 + 1}{4\alpha} \right) + O(\omega_m^2) \quad (18)$$

One can easily verify that the inclusion of fermionic self-energy $\Sigma(k, \omega_m) \propto i \text{sgn}(\omega_m)$ will not change the polarization operator, i.e., $\Pi(\Omega_m)$ retains the same form even if we compute it using dressed fermions.

To verify self-consistency of the calculations, we also computed the self-energy away from the FS. We found $\Sigma(k_{\perp}, 0) \propto (1/N)v_F k_{\perp} \log(\Lambda/|v_F k_{\perp}|)$, where Λ is the upper cutoff in momentum integration. The presence of the logarithm implies that Fermi velocity also acquires singular renormalization at CDW QCP (Refs. 11 and 52). This singularity breaks self-consistency of one-loop calculation of fermionic and bosonic self-energies if we keep N finite, but self-consistent procedure still remains rigorously justified at this loop order if we set $N \rightarrow \infty$. The situation gets more complex at higher loop orders due to special role of forward scattering and backscattering processes which give rise to the dependence of Σ on k_{\perp} without the factor $1/N$ (Refs. 48, 50, 56, and 57). How important are these effects in unclear and in this work we restrict with one-loop self-energy.

B. The pairing problem

We now use the normal state results as inputs for the analysis of the pairing mediated by CDW fluctuations with momenta around Q_x and Q_y . To leading order in $1/N$, the pairing problem can be analyzed without vertex corrections, by summing up the ladder series of diagrams in the particle-particle channel^{11,52}.

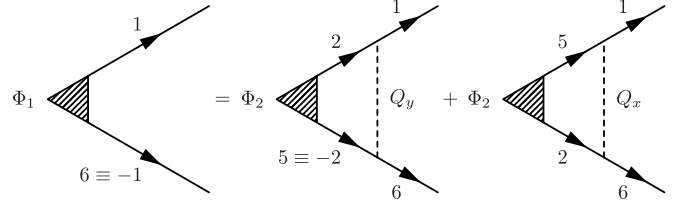


FIG. 5. Diagrammatic representation of the coupled ladder equations for superconducting order parameters Φ_1 and Φ_2 , which involve fermions in hot regions 1 and 2 in Fig. 1.

We first focus on the momentum region where hot spots 1,2, and 5 = -2, and 6 = -1 are located (see Fig. 3). We introduce superconducting order parameters $\Phi_1 \sim \langle c_1 c_6 \rangle = \langle c_1 c_{-1} \rangle$ and $\Phi_2 \sim \langle c_2 c_5 \rangle = \langle c_2 c_{-2} \rangle$ and obtain in the standard way a set of coupled gap equations for the two condensates. The interactions with momentum transfer $Q_x = (Q, 0)$ and $Q_y = (0, Q)$ connect hot spots 1,5 with 2,6, and hot spots 1,2 with 5,6, correspondingly. As the consequence, the interactions relate Φ_1 with Φ_2 and vice versa. We show the equation for Φ_1 diagrammatically in Fig. 5. In analytical form, we have

$$\Phi_1(k) = T \sum_{k'} U_c^{\text{eff}}(k - k') \times [G_2(k')G_5(-k')\Phi_2(k') + G_2(-k')G_5(k')\Phi_2(-k')] \quad (19)$$

where $k = (\omega_m, \mathbf{k})$ and $k' = (\omega'_m, \mathbf{k}')$ and \mathbf{k}, \mathbf{k}' are momentum deviations from the corresponding hot spots. The fermionic Green's function are given by $G_i(k) = 1/[i\omega_m - \epsilon_i(\mathbf{k}) + \Sigma_i(k)]$. The equation for Φ_2 in terms of Φ_1 has the same form, and thus Φ_1 and Φ_2 have the same magnitude.

Because the two kernels in the Eq. (19) (the prefactors for Φ_2 in the right hand side) are both positive (we recall that U_{eff} is positive), the $U(1)$ order parameters Φ_1 and Φ_2 have the same phase, i.e., $\Phi_1 = \Phi_2$. By the same token, the SC order parameters in the momentum range near hot spots 3,4,7,8, namely $\Phi_3 \sim \langle c_3 c_8 \rangle = \langle c_3 c_{-3} \rangle$ and $\Phi_4 \sim \langle c_4 c_7 \rangle = \langle c_4 c_{-4} \rangle$ are also equal. The kernels of the gap equations in the regions 1,2,5,6 and 3,4,7,8 are the same, hence the magnitudes of $\Phi_1 = \Phi_2$ and $\Phi_3 = \Phi_4$ are identical. However, there is no specification of the relative phase between superconducting order parameters in the two regions. Setting aside more exotic possibilities of phase difference equal to a fraction of π , we are left with two options for the pairing symmetry: an s -wave, for which the phases of Φ_1 and Φ_3 are identical, and a $d_{x^2-y^2}$, for which $\Phi_3 = -\Phi_1$ (see Fig. 3). When only CDW-mediated interaction is considered, the two pairing states are degenerate. This has been noticed before⁴⁰, and it was argued that the degeneracy is lifted by other interactions, e.g., antiferromagnetic spin fluctuations would favor d -wave.

We now proceed with the calculation of T_c^{ch} . We assume and then verify that the $\Phi_1(k) = \Phi_2(k) = \Phi(k)$ are even functions of momentum \mathbf{k} . The linearized gap equation (19), whose solution exists right at $T = T_c$, then becomes

$$\Phi(k) = 2T \sum_{k'} |U_c^{\text{eff}}(k - k')| G_2(k') G_5(-k') \Phi(k'). \quad (20)$$

In the right hand side of Eq. (20) we first integrate over momentum transverse to the FS. Neglecting terms small in $1/N$, we obtain

$$\begin{aligned} \Phi(\omega_m, k_{\parallel}) &= \frac{\bar{g}_c T}{v_F} \sum_{m'} \int \frac{dk'_{\parallel}}{2\pi} \frac{\Phi(\omega'_m, k'_{\parallel})}{|\omega'_m - i\Sigma(\omega'_m, k'_{\parallel})|} \\ &\times \frac{1}{k_{\parallel}^2 + k'_{\parallel}{}^2 - 2\beta k_{\parallel} k'_{\parallel} + \gamma_c |\omega_m - \omega'_m|}, \quad (21) \end{aligned}$$

where $\beta = (1 - \alpha^2)/(1 + \alpha^2)$. This factor appears in the last term in (21) because k_{\parallel} and k'_{\parallel} are parallel components of momenta in *different* segments of the FS, namely near hot spots 1 and 2, respectively.

A similar gap equation has been analyzed in the context of spin-mediated pairing near SDW QCP^{11,46,52}. To

make this paper self-contained, we present some details of the computation of T_c^{ch} in our case.

It is usually more convenient not to solve Eq. (21) directly, but to add to the right hand side of the gap equation an infinitesimal pairing condensate Φ_0 and compute pairing susceptibility $\chi_{pp} = \Phi/\Phi_0$. The transition temperature T_c is the one at which pairing susceptibility diverges. This approach has an advantage in that the pairing susceptibility can be analyzed within perturbation theory.

The first iteration gives

$$\Phi(\omega_m \sim T, 0) = \Phi_0 \left(1 + \frac{l}{2\pi} \log^2 \frac{\omega_{0c}}{T} \right), \quad l = \frac{2\alpha}{\alpha^2 + 1}, \quad (22)$$

where, we remind, $\omega_{0c} \sim \bar{g}_c$ is the upper edge of NFL behavior. We note that neither the coupling constant \bar{g}_c nor $1/N$ directly appear in Eq. (22), i.e., once temperature is expressed in units of ω_{0c} , the renormalization of Φ_0 is fully universal. The presence of \log^2 term (i.e., one extra power of \log compared to BCS theory) is the consequence of the singular dependence of the fermionic self-energy on momentum along the FS. The \log^2 term comes from momentum range where $\Sigma(\omega_m, k_{\parallel}) \sim i\omega_m/|k_{\parallel}|$ [see Eq. (18)]. At $\bar{g}_c/v_F \gg |k_{\parallel}| \gg \sqrt{\gamma_c |\omega_{0c}|}$ the term $1/|\omega'_m - i\Sigma(\omega'_m, k'_{\parallel})|$ in Eq. (21) scales as $|k_{\parallel}|/\omega_m$. To logarithmic accuracy, the momentum integral over k'_{\parallel} in Eq. (21) yields $\int_{\gamma_c |\omega'_m|} dk'_{\parallel}/k'_{\parallel} \propto \log |\omega'_m|$, and the frequency integral over ω'_m then yields $\int_T (\log |\omega'_m|)/|\omega'_m| d\omega'_m \propto \log^2(1/T)$. For the spin-fermion model, this result was first obtained in Ref. 11.

The $\log^2 T$ renormalization of the pairing vertex has been found in other contexts⁵⁸⁻⁶¹. To see how it is relevant for T_c one has to go beyond one loop order. To get the insight, we first consider the ‘‘weak coupling’’ limit by formally replacing the actual coupling $l = 2\alpha/(\alpha^2 + 1)$ by an effective $l_{\epsilon} = 2\epsilon\alpha/(\alpha^2 + 1)$ and taking the limit $\epsilon \ll 1$. In this limit, series of \log^2 renormalizations can be summed up explicitly, and the result is $\Phi = \Phi_0 e^{l_{\epsilon}/(2\pi) \log^2(\omega_{0c}/T)}$. We see that, at the \log^2 level, the pairing susceptibility does increase with decreasing T , but it does not diverges at any finite T . One then has to go beyond the \log^2 approximation and include subleading $O(\log)$ terms. In the weak coupling limit $\epsilon \ll 1$ this can be done rigorously, along the lines specified in Ref. 46, and the result is that subleading $O(\log)$ terms do give rise to the divergence of the pairing susceptibility at a finite T_c^{ch} given by

$$T_c^{\text{ch}} \sim \omega_{0c} e^{-1/\epsilon}. \quad (23)$$

The exponential dependence is the same as in BCS formula, which is not accidental because in the limit $\epsilon \ll 1$ the main contribution to superconductivity comes from fermions away from the hot regions, where self-energy has FL form. However, in distinction to BCS formula, the prefactor ω_{0c} is not the upper cutoff for the attraction but rather the scale set by the coupling constant \bar{g}_c . The proportionality of T_c^{ch} to the coupling \bar{g}_c is the fingerprint of the pairing near a quantum-critical point^{47,62}.

For the physical case $\epsilon = 1$, we expect from (23) $T_c^{\text{ch}} \sim \omega_{0c}$. To obtain the exact relation we solved Eq. (21) directly, using the finite-temperature form of the fermionic self-energy. Typical internal momenta and typical internal frequency are of order, $k_{\parallel}^2 \sim \gamma_c \omega_m \sim \gamma \omega_{0c}$ and $\omega \sim \omega_{0c}$. In this situation, fermions from both NFL and FL regions contribute to the pairing. For numerical evaluation of T_c^{ch} we extracted the fermionic dispersion in hot regions from ARPES data for $\text{Bi}_2\text{Sr}_2\text{CaCu}_2\text{O}_{8+x}$ (Ref. 63) and obtained $\alpha = 0.074$. Using this value for α

we obtained numerically

$$T_c^{\text{ch}} = 0.0025 \bar{g}_c. \quad (24)$$

For comparison, in the spin-fermion model the critical temperature at SDW QCP is⁴⁶ $T_c^{\text{sp}} = 0.0073 \bar{g}_s$ ($T_c^{\text{sp}} \sim 140$ K for $\bar{g}_s \sim 1.7$ eV). We see that T_c in spin-fermion and charge-fermion models on top of the corresponding QCP are comparable if $\bar{g}_c \geq \bar{g}_s$. If this is the case, then CDW fluctuations give rise to substantial enhancement of the superconducting T_c around CDW QCP. One also should keep in mind that the result we quoted for T_c^{sp} due to spin fluctuation exchange is T_c^{sp} right on top of SDW QCP. Near the CDW QCP, magnetic ξ_s is finite and spin-mediated T_c^{sp} is reduced.

Away from the CDW QCP, charge-fluctuation exchange preserves FL behavior and charge-mediated T_c drops and eventually follows weak coupling BCS formula. The self-energy at a finite charge correlation length ξ_c is modified compared to Eq. (16) and is given by

$$\Sigma(k_{\parallel}, \omega_m) = \frac{i\bar{g}_c}{\pi v_F \gamma_c} \text{sgn}(\omega_m) \left[\sqrt{\gamma_c |\omega_m| + \left(\frac{2\alpha k_{\parallel}}{\alpha^2 + 1}\right)^2 + \xi_c^{-2}} - \sqrt{\left(\frac{2\alpha k_{\parallel}}{\alpha^2 + 1}\right)^2 + \xi_c^{-2}} \right]. \quad (25)$$

Now even right at a hot spot (at $k_{\parallel} = 0$) the self-energy has a FL form

$$\Sigma(\omega_m, 0) = \lambda_c (i\omega_m) - i \frac{\omega_m^2}{4\omega_{\text{cf}}}, \quad (26)$$

where

$$\lambda_c = \frac{\bar{g}_c \xi_c}{2\pi v_F}, \quad \text{and} \quad \omega_{\text{cf}} = \frac{\xi_c^{-2}}{\gamma_c} = \frac{\bar{g}_c}{4\pi \lambda_c^2} \frac{\alpha}{\alpha^2 + 1}. \quad (27)$$

The dimensionless charge fermion coupling λ_c (the ratio of \bar{g}_c to typical fermionic energy $v_F \xi_c^{-1}$) decreases when ξ_c decreases. Once $\lambda_c \leq 1$, charge-relaxation scale ω_{cf} becomes the upper energy cutoff for the pairing, and T_c follows BCS-Eliashberg-McMillan formula⁶⁴

$$T_c \sim \omega_{\text{cf}} e^{-\frac{1+\lambda_c}{\lambda_c}}. \quad (28)$$

We present the numerical result for the behavior of T_c^{ch} as a function of ξ_c in Fig. 11 (red line). A similar reduction of charge-mediated T_c^{ch} is expected on the other side of CDW QCP, in the charge-ordered state.

III. CHARGE-FERMION COUPLING CONSTANT FROM THE SPIN-FERMION MODEL

To compare the magnitudes of \bar{g}_c and \bar{g}_s we compute their ratio within a particular microscopic model for

charge order in the cuprates. Namely, we assume, as in earlier works by several groups including us^{11,12,52,62,65-68} that spin fluctuations develop at higher energies than CDW (and superconducting) fluctuations, and CDW order emerges due to spin-fluctuation exchange, as a composite order.

To this end, we consider a 2D itinerant electron system in which the primary interaction between fermions is mediated by soft collective spin fluctuations at the antiferromagnetic momentum $\mathbf{Q}_{\pi} = (\pi, \pi)$. Such an interaction, shown as the wavy line in Fig. 6, scatters fermions between hot spots 2 and 4, 1 and 3, etc, and is proportional to the dynamical spin susceptibility:

$$\mathcal{H}_{\text{eff}} = -U_s^{\text{eff}}(\mathbf{q}, \Omega_m) \sum_{k,p} c_{k,\alpha}^{\dagger} \vec{\sigma}_{\alpha\beta} c_{k+q,\beta} c_{p,\gamma}^{\dagger} \vec{\sigma}_{\gamma\delta} c_{p-q,\delta} \quad (29)$$

where

$$U_s^{\text{eff}}(\mathbf{q}, \Omega_m) = g_s^2 \chi_s(\mathbf{q}, \Omega_m) = \frac{\bar{g}_s}{\xi_s^{-2} + (\mathbf{q} - \mathbf{Q}_{\pi})^2 + \gamma_s |\Omega_m|}, \quad (30)$$

where γ_s is the corresponding Landau damping coefficient and the scale \bar{g}_s sets the magnitude of T_c^{sp} for spin-mediated superconductivity.

Except for special cases, there is no rigorously justified procedure to obtain Eq. (29) starting from a model of fermions interacting with some short-range interaction

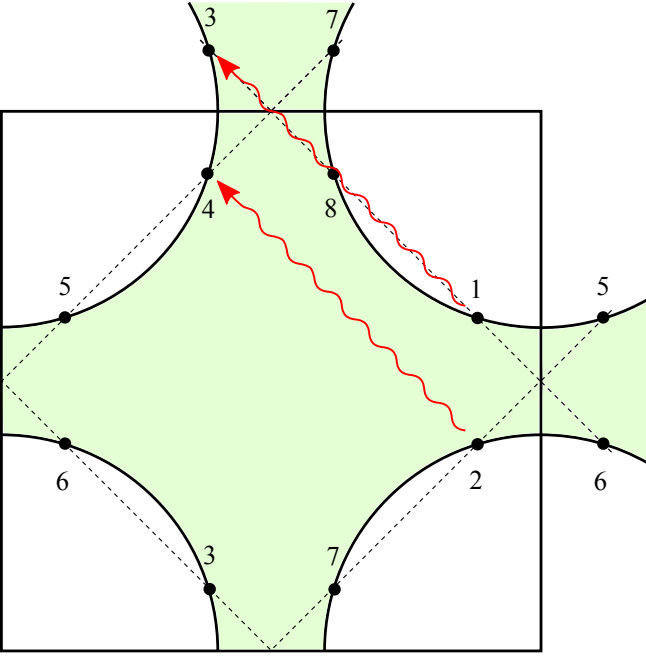


FIG. 6. Schematic representation of spin-mediated interaction. Near an antiferromagnetic quantum-critical point in a metal hot fermions scatter into each other by exchanging soft antiferromagnetic spin fluctuations with momentum (π, π) (the wavy lines).

$U(r)$ because the main contribution to static part of U_s^{eff} comes from fermions with high energies.

One commonly used approach is to treat static part of spin-mediated interaction phenomenologically and just postulate Ornstein-Zernike form of the static $\chi_s(\mathbf{q}, 0)$ (this is the same procedure that we used in the charge-fermion model). Once the model with static spin-mediated interaction is established, one can compute the dynamical part of $\chi_s(\mathbf{q}, \Omega_m)$ (the Landau damping term) within this model, as it comes from fermions with small energies. Within this approach, one cannot relate \bar{g}_s with $U(r)$, but one can express Landau damping coefficient γ_s via \bar{g}_s . The relation is⁵² $\gamma_s = 2\bar{g}_s[2/(\pi v_F^2)]$, where for comparison with RPA below we pulled out factor of 2 due to spin summation.

A complementary approach is to treat U_s^{eff} as the charge component of the fully renormalized vertex function $\Gamma_{\alpha\gamma, \beta\delta}(\mathbf{q}, \Omega_m)$ at momentum transfer \mathbf{q} near \mathbf{Q}_π . The vertex function Γ is the opposite of physical antisymmetrized interaction (a direct interaction minus the one with outgoing fermions interchanged). The vertex function can be obtained in RPA by summing up particular ladder and bubble diagrams which form geometrical series (for details see Ref. 69). The approach is best understood when $U(r)$ is approximated as on-site Hubbard interaction U . The RPA gives

$$\begin{aligned} \Gamma_{\alpha\gamma, \beta\delta}(\mathbf{q}, \Omega_m) &= -\frac{U}{1 - U^2\Pi^2(\mathbf{q}, \Omega_m)}\delta_{\alpha\beta}\delta_{\gamma\delta} + \frac{U}{1 - U\Pi(\mathbf{q}, \Omega_m)}\delta_{\alpha\delta}\delta_{\beta\gamma} \\ &= -\frac{U}{2(1 + U\Pi(\mathbf{q}, \Omega_m))}\delta_{\alpha\beta}\delta_{\gamma\delta} + \frac{U}{2(1 - U\Pi(\mathbf{q}, \Omega_m))}\vec{\sigma}_{\alpha\beta} \cdot \vec{\sigma}_{\gamma\delta} \end{aligned} \quad (31)$$

where to split the vertex into spin and charge parts we used $\vec{\sigma}_{\alpha\beta} \cdot \vec{\sigma}_{\gamma\delta} = -\delta_{\alpha\beta}\delta_{\gamma\delta} + 2\delta_{\alpha\delta}\delta_{\beta\gamma}$. For a repulsive interaction $U > 0$, and the interaction in the spin channel is enhanced and at large enough U diverges at \mathbf{q} , at which static $\Pi(\mathbf{q}, 0) > 0$ is at maximum. We assume that the maximum of $\Pi(\mathbf{q}, 0)$ is at $\mathbf{q} = \mathbf{Q}_\pi$.

Near $\Pi(\mathbf{Q}_\pi, 0) = 1/U$, the interaction in the spin channel well exceeds the one in the charge channel, and one can keep only the spin component of the interaction, i.e., approximate the dressed interaction by Eq. (29) with

$$U_s^{\text{eff}}\vec{\sigma}_{\alpha\beta} \cdot \vec{\sigma}_{\gamma\delta} = \frac{U}{2(1 - U\Pi(\mathbf{q}, \Omega_m))}\vec{\sigma}_{\alpha\beta} \cdot \vec{\sigma}_{\gamma\delta}. \quad (32)$$

Expanding the polarization operator near antiferromagnetic momentum and zero frequency, we obtain

$$\Pi(\mathbf{q}, \Omega_m) = \Pi(\mathbf{Q}_\pi, 0) - C_\pi(\mathbf{q} - \mathbf{Q}_\pi)^2 - \frac{2|\Omega_m|}{\pi v_F^2} \quad (33)$$

(the last term comes from fermions near the FS and the prefactor for Ω_m term is known exactly). Substituting

this form into (32) we obtain after simple manipulations the same $U_s^{\text{eff}}(\mathbf{q}, \Omega_m)$ as in Eq. (30) with

$$\bar{g}_s = \frac{1}{2C_\pi}, \quad \xi_s^{-2} = \frac{1 - U\Pi(\mathbf{Q}_\pi, 0)}{UC_\pi}, \quad \gamma_s = 2\bar{g}_s \frac{2}{\pi v_F^2} \quad (34)$$

We see that the expression for the Landau damping coefficient is exactly the same as in the other (semi-phenomenological) approach, the only new element of RPA is that $\bar{g}_s = 1/(2C_\pi)$ is related to the behavior of the static polarization bubble. Formally, \bar{g}_s doesn't depend on U , but in reality C_π is of the same order as $\Pi(\mathbf{Q}_\pi, 0)$ (in units where lattice constant $a = 1$), and the latter is approximately $1/U$ near a SDW QCP. As a result, \bar{g}_s is fact is of order U .

The interaction mediated by spin fluctuations gives rise to d -wave superconductivity and to fermionic self-energy. In the FL regime, $\Sigma(\omega_m) \approx \lambda_s \omega_m$, where $\lambda_s = 3\bar{g}/(4\pi v_F \xi_s^{-1})$. This self-energy gives rise to mass renormalization $m^*/m = 1 + \lambda_s$ and to quasiparticle residue $1/Z = 1/(1 + \lambda_s)$. We will include this renor-

malization into the calculations below.

We now proceed to construct the interaction in the CDW channel.

The CDW instability with the ordering momentum $Q_x = (Q, 0)$ and $Q_y = (0, Q)$ emerges in this approach as a preliminary collective instability at a finite ξ_s , due to spin-fluctuation exchange. A way to obtain CDW instability is to introduce infinitesimal CDW field Δ_k^Q , which couples to incommensurate component of charge density as $\Delta_k^Q c_{k-Q/2,\alpha}^\dagger \delta_{\alpha\beta} c_{k+Q/2,\beta}$, and compute susceptibility with respect to this field. This has been done^{13,14,17} by summing up ladder series of renormalizations due to spin-fluctuation exchange. Each act of spin-fluctuation exchange transforms hot fermions near, say, hot points 1 and 2 in Fig. 6 into another set of hot fermions near the points 3 and 4. The set 3,4 is generally different from the set 1,2 (because directions of the Fermi velocities are different), so to obtain the susceptibility one has to solve the set of two coupled equations for fully renormalized Δ_k^Q with the center of mass momentum \mathbf{k} either between points 1 and 2 or between points 3 and 4.

There is no rigorous justification why one should restrict with only ladder diagrams, even at large N . The first non-ladder diagram is small numerically, but not parametrically, compared to the ladder diagram of the same loop order. Accordingly, there is no point to keep N as artificially large parameter, and in this section we set the number of pairs of hot spots N to their actual value $N = 4$.

We present the diagrammatic representation of this set of equations in Fig. 7(a,b). The linear “gap” equation for Δ_k^Q has been analyzed in Ref. 14 and the outcome is that the CDW susceptibility diverges at a finite T_{cdw} before the system develops CDW order. The critical temperature T_{cdw} decreases as ξ_s decreases and vanishes at a finite critical ξ_s , setting up a CDW QCP at some distance away from SDW QCP²¹ (see Fig. 1).

Alternatively, one can combine pairs of subsequent renormalizations of Δ_k^Q into new effective interaction at *small* momentum transfer [see Fig. 7(c)], which we label as U_c and show graphically in Fig. 8. This composite effective interaction is the convolution of two fermionic propagators and two spin-fluctuation propagators. Explicit calculation shows^{21,70} that U_c is numerically smaller but parameter-wise of the same order as a single spin-fluctuation propagator – one extra power of \bar{g}_s in the numerator gets cancelled out by the Landau damping coefficient $\gamma_s \propto \bar{g}_s$ in the denominator. This effective interaction is repulsive ($U_c > 0$) because the polarization bubble in the particle-hole channel is negative, as opposed to the bubble in the particle-particle channel.

The corresponding term in the Hamiltonian is

$$\mathcal{H}_c = U_c (c_{2,\alpha}^\dagger c_{2,\nu})(c_{1,\mu}^\dagger c_{1,\beta}) \left[\frac{9}{2} \delta_{\alpha\beta} \delta_{\mu\nu} + \frac{1}{2} \vec{\sigma}_{\alpha\beta} \cdot \vec{\sigma}_{\mu\nu} \right], \quad (35)$$

where subindices 1 and 2 indicate that the corresponding

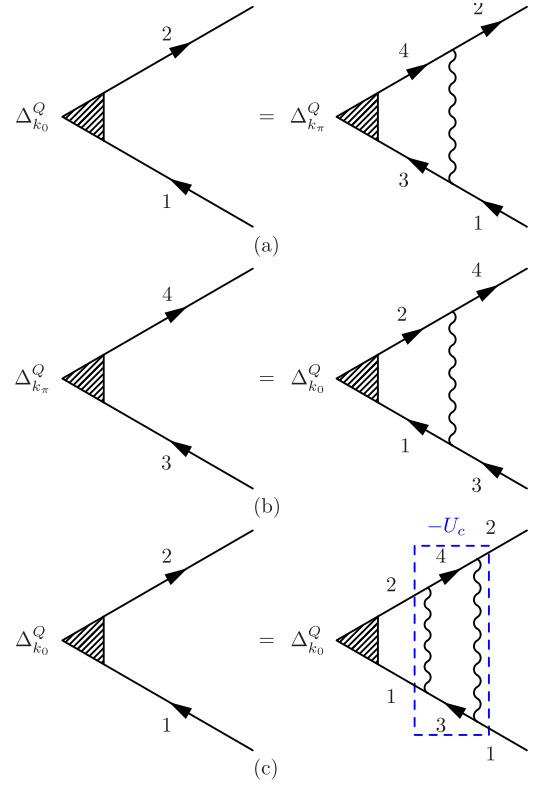


FIG. 7. The linearized “gap” equation for the CDW order parameter $\Delta_k^Q \sim \langle c_{k+Q/2}^\dagger c_{k-Q/2} \rangle$. We define the center-of-mass momentum of hot spots 1 and 2 as k_0 and that of hot spots 3 and 4 as k_π . Panels (a) and (b): the coupled gap equations for $\Delta_{k_0}^Q$ and $\Delta_{k_\pi}^Q$. Panel (c): The gap equation for $\Delta_{k_0}^Q$ only, obtained by combining panels (a) and (b). We treat the composite object in the dashed frame as the effective interaction U_c (the prefactor -1 reflects that interaction appears in the diagram with the minus sign).

momenta are near hot spots 1 and 2, and the spin factors originate from

$$\begin{aligned} & (\vec{\sigma}_{\gamma\beta} \cdot \vec{\sigma}_{\alpha\delta}) (\vec{\sigma}_{\mu\gamma} \cdot \vec{\sigma}_{\delta\nu}) \\ &= \left(\frac{3}{2} \delta_{\alpha\beta} \delta_{\gamma\delta} - \frac{1}{2} \vec{\sigma}_{\alpha\beta} \cdot \vec{\sigma}_{\gamma\delta} \right) \left(\frac{3}{2} \delta_{\delta\gamma} \delta_{\mu\nu} - \frac{1}{2} \vec{\sigma}_{\delta\gamma} \cdot \vec{\sigma}_{\mu\nu} \right) \\ &= \frac{9}{2} \delta_{\alpha\beta} \delta_{\mu\nu} + \frac{1}{2} \vec{\sigma}_{\alpha\beta} \cdot \vec{\sigma}_{\mu\nu}. \end{aligned} \quad (36)$$

Only the first, $\frac{9}{2} \delta_{\alpha\beta} \delta_{\mu\nu}$ term is relevant to CDW instability as it renormalizes Δ_k^Q , which acts between fermions near hot spots 1 and 2, with the same spin components (i.e., it is convoluted with $\delta_{\alpha\beta}$), therefore we can drop the $\frac{1}{2} \vec{\sigma}_{\alpha\beta} \cdot \vec{\sigma}_{\mu\nu}$ component in Eq. (35).

The composite interaction U_c can be approximated as a constant if the deviation of the fermionic momenta from corresponding hot spots (e.g., regions 1 and 2 in Fig. 6) are smaller than the inverse spin correlation length ξ_s^{-1} . At larger deviations from hot spots, U_c becomes function of momenta and decreases.

We now turn to the calculation of the fermionic self-energy and pairing instability. At a first glance, an-

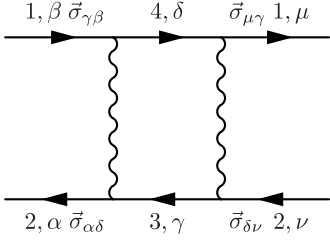


FIG. 8. The diagrammatic representation of the composite effective interaction U_c (same as in the dashed frame in Fig. 7). This effective interaction is a convolution of a particle-hole bubble and two antiferromagnetic spin-fluctuation propagators.

teraction with a positive (repulsive) U_c cannot give rise to the pairing instability with sign-preserving gap between the regions 1 and 2. On a more careful look, however, we notice that the interaction in Eq. (35) is the one at small momentum transfer (both incoming and outgoing fermions are near the same hot spot), while to analyze CDW-mediated pairing (Fig. 5) and fermionic self-energy (Fig. 4(c)) one needs density-density interaction at momentum transfer approximately equal to the momentum difference between hot spots 1 and 2, namely, $Q_y = (0, Q)$. To obtain this interaction, we need to interchange one creation and one annihilation fermionic operator. Then we obtain from Eq. (35)

$$\mathcal{H}_c = -\frac{9U_c}{2}(c_{2,\alpha}^\dagger \delta_{\alpha\beta} c_{1,\beta})(c_{1,\mu}^\dagger \delta_{\mu\nu} c_{2,\nu}). \quad (37)$$

Viewed this way, the effective interaction is *attractive* and is capable to give rise to pairing.

Another, more standard way to verify that the density-density interaction with momentum transfer \mathbf{Q} is attractive is to again extract it from the vertex function $\Gamma_{\alpha\mu,\beta\nu}(\mathbf{q}, \Omega_m)$. To second order in the spin-fluctuation propagator, there are two direct and two anti-symmetrized diagrams for $\Gamma_{\alpha\mu,\beta\nu}(\mathbf{q}, \Omega_m)$ which contain spin propagators with momenta near \mathbf{Q}_π . We show them in Fig. 9. In evaluating these four diagrams, we additionally require that both spin-fluctuation propagators carry the same momenta, as only then one can cancel extra power of \bar{g}_s . It is easy to show that only the fourth diagram (the one from the anti-symmetrized part) satisfies these conditions. This diagram is exactly the same as the one in Fig. 8, but there is an extra minus sign in front of it. The evaluation of the diagram itself gives $-U_c$ because particle-hole bubble is negative. The extra (-1) in front of this diagram cancels the overall minus sign. As a result, the charge component of the vertex function becomes

$$\Gamma_{\alpha\mu,\beta\nu}^c = \frac{9U_c}{2} \delta_{\alpha\beta} \delta_{\mu\nu} \quad (38)$$

where the spin structure is obtained the same way as in Eq. (36). Associating the charge component of the vertex function with the effective density-density interaction, we reproduce Eq. (37).

The effective interaction $-(9U_c/2)c_{2,\alpha}^\dagger c_{1,\alpha} c_{1,\mu}^\dagger c_{2,\mu}$ is the *bare* interaction at momentum transfer Q_y , and in this respect $9U_c/2$ plays the same role as Hubbard U played for our earlier derivation of spin-mediated interaction within RPA. Just like we did for spin case, we now dress interaction by summing up series of RPA diagrams (see Fig. 10). This way we obtain fully renormalized (within RPA) effective interaction in the charge channel

$$U_c^{\text{eff}} = \frac{9U_c}{2} \frac{1}{1 - 9U_c |\Pi_c(\mathbf{q}, \Omega_m)|} \quad (39)$$

Expanding the polarization operator Π_c near, say $\mathbf{Q} = Q_y$, we obtain

$$|\Pi_c(\mathbf{q}, \Omega_m)| = |\Pi(Q_y, 0)| - C_y(\mathbf{q} - \mathbf{Q}_y)^2 - \frac{|\Omega_m|}{\pi v_F^2} \frac{\alpha^2 + 1}{2\alpha} \quad (40)$$

Substituting this form into (39) we obtain the effective charge-mediate interaction the same form as in Eq. (8) with

$$\bar{g}_c = \frac{1}{2C_y}, \quad \xi_c^{-2} = \frac{1 - 9U_c \Pi(Q_y, 0)}{9U_c C_y}, \quad \gamma_c = \bar{g}_c \frac{1}{\pi v_F^2} \frac{\alpha^2 + 1}{\alpha} \quad (41)$$

To proceed further we approximate the dynamical spin susceptibility $\chi_s(\mathbf{q}, \Omega_m)$ by its value at $\mathbf{q} = \mathbf{Q}_\pi$ and $\Omega_m = 0$ and integrate over fermions within the momentum range of the width Λ around hot spots. Like we said above, the approximation of U_c by a constant is valid when momentum deviations from a hot spot are at most of order ξ_s^{-1} , so $\Lambda \xi_s$ is generally of order one. We also assume for simplicity that CDW order parameter has a pure d -wave form, i.e., set our parameter α to be one. Within this last approximation, the polarization operator has the same form between points 1-2 and 3-4. Evaluating the polarization operator Π_c we then find near $\mathbf{q} = \mathbf{Q}_y$ ¹⁷

$$|\Pi_c(\mathbf{q})| = \frac{\Lambda}{\sqrt{2}\pi^2 v_F (1 + \lambda)} \left[1 - \tilde{C}_y \frac{(\mathbf{q} - \mathbf{Q}_x)^2}{\Lambda^2} \right] \quad (42)$$

where \tilde{C}_y is of order one and we remind that $\lambda = 3\bar{g}_s/(4\pi v_F \xi_s^{-1})$ is the mass renormalization due to spin-fluctuation exchange. The variable C_y , which we introduced in (40) is related to \tilde{C}_y as

$$C_y = \tilde{C}_y \frac{1}{\sqrt{2}\pi^2 v_F (1 + \lambda) \Lambda}. \quad (43)$$

Within the same approximation the composite interaction U_c is given by

$$U_c = (\bar{g}_s \xi_s^2)^2 |\Pi_c(\mathbf{Q}_y)| = \bar{g}_s^2 \xi_s^3 \frac{\Lambda \xi}{\sqrt{2}\pi^2 v_F (1 + \lambda)} \quad (44)$$

such that

$$9U_c |\Pi_c(\mathbf{Q}_y)| = (3\bar{g}_s \xi_s^2)^2 \frac{(\Lambda \xi)^2}{2\pi^4 v_F^2 (1 + \lambda)^2} \quad (45)$$

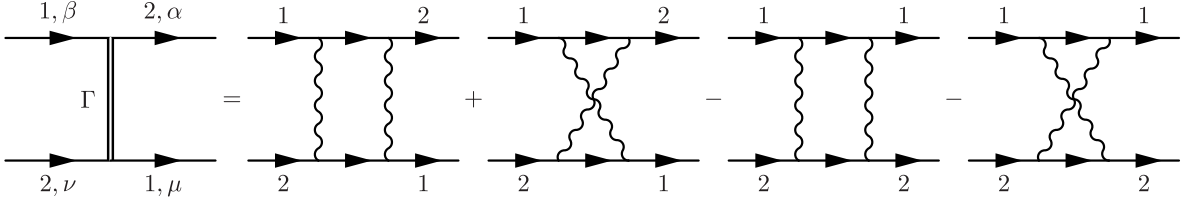


FIG. 9. The vertex function with momentum transfer near Q_y in two-loop order (two spin-fluctuation propagators). Other two-loop diagrams (not shown) contain spin-fluctuation propagators with small momentum transfer and are irrelevant for our purposes. The charge component of this vertex function is $9U_c/2$. The opposite of this charge component (i.e., $-9U_c/2$) is the bare interaction in the charge channel at momentum transfer near Q_x or Q_y .

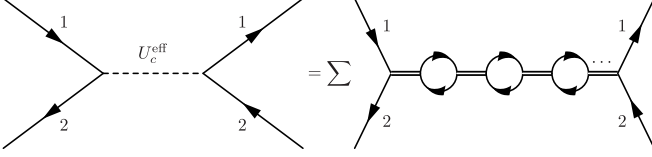


FIG. 10. The RPA diagrams for the dressed effective charge interaction U_c^{eff} . Each double solid line is the "bare" U_c – the charge component of the vertex function at two-loop order. The dressed interaction U_c^{eff} can be viewed as charge fluctuation exchange (see text).

Using the condition $9U_c|\Pi_c(\mathbf{Q}_y)| \approx 1$, we eliminate unknown scale Λ and obtain

$$C_y = \tilde{C}_y \frac{3\bar{g}_s \xi_s^2}{2\pi^4 v_F^2 (1+\lambda)^2} \quad (46)$$

Hence

$$\bar{g}_c = \frac{1}{2C_y} = \bar{g}_s \frac{3\pi^2}{16\tilde{C}_y} \left(\frac{1+\lambda}{\lambda}\right)^2 \approx 2\bar{g}_s \frac{1}{\tilde{C}_y} \left(\frac{1+\lambda}{\lambda}\right)^2 \quad (47)$$

We see that within this approximation the ratio \bar{g}_c/\bar{g}_s depends on the value of dimensionless parameter \tilde{C}_y . To obtain this parameter one needs to know more precisely system behavior at energies comparable to Λ . Still, if $\tilde{C}_y(\lambda/(1+\lambda))^2 \leq 1$, then $\bar{g}_c \geq 2\bar{g}_s$, in which case superconducting T_c^{ch} from the exchange of near-critical charge fluctuations will may exceed T_c^{sp} from the spin-fluctuation exchange. This is the central result of this section.

A more quantitative analysis requires extensive numerical calculations and is beyond the scope of this work. We also emphasize that there is no known controllable procedure of the derivation of the effective interaction mediated by near-critical collective bosonic fluctuations, the RPA which we used is an uncontrollable approximation. And we also recall that the composite interaction U_c (the convolution of two fermionic propagators and two spin propagators) does depend on external momenta and frequency, and already the calculation of T_{cdw} requires one to solve integral equation for momentum and frequency dependent full Δ_k^Q .

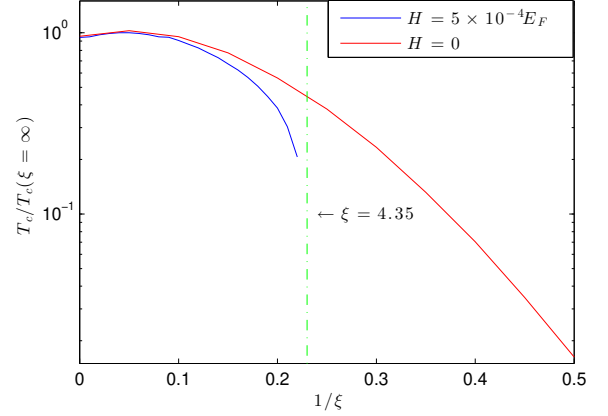


FIG. 11. The behavior of T_c^{ch} 's as a function of $1/\xi_c$ with and without an external field H , obtained by explicitly solving Eq. (48). Without a magnetic field T_c^{ch} decreases as ξ_c becomes finite and at small enough ξ_c crosses over from quantum-critical to BCS-like behavior [see Eq. (28)]. At a finite field, T_c^{ch} at $\xi_c = \infty$ is somewhat reduced, but, most important, T_c^{ch} now vanishes at a finite ξ_c^{cr} . In numerical calculations we used $\bar{g}_c = 0.75E_F$, $\alpha = 0.076$, and $\mu_B H = 5 \times 10^{-4}E_F$ (for $E_F = 1$ eV, this H is ~ 10 Tesla). For these parameters, $\xi_c^{\text{cr}} = 4.35/k_F$. The critical ξ_c^{cr} is well described by Eq. (50) – plugging ξ_c^{cr} into this equation gives 1.2 in the right hand side, close enough to the actual 1.

IV. SHRINKING OF A SUPERCONDUCTING DOME IN A MAGNETIC FIELD

Finally, we discuss the issue of how T_c^{ch} , mediated by collective degrees of freedom, evolves in the presence of an external magnetic field. For definiteness, we focus on the role of near-critical charge fluctuations and neglect the contribution to T_c from spin fluctuations.

It has been found experimentally^{33,71} that in the presence of a magnetic field H superconducting T_c , viewed as a function of doping, splits into two domes, and the one at higher doping is centered at or very near CDW QCP. As H increases, the maximum of T_c in this dome is somewhat reduced, but, most notably, the width of the dome shrinks, i.e., superconductivity get progressively confined to a CDW QCP.

We show that this behavior is reproduced within a quantum-critical CDW pairing scenario. The argument is rather straightforward – right at CDW QCP, T_c^{ch} is set by charge-fermion coupling \bar{g}_c , and to reduce T_c^{ch} one would need to apply a rather strong magnetic field $\mu_B H \sim \bar{g}_c$. Away from CDW QCP, in the FL regime, T_c^{ch} is reduced and eventually follows BCS formula. In the latter case, a much weaker $\mu_B H$ is needed to kill superconductivity.

To see how this works in practice, we solved for charge-mediated T_c^{ch} at a finite charge correlation length ξ_c by assuming that the dominant effect of the field is Zeeman splitting of fermionic energies in the particle-particle bubble. Within this approximation, the linearized integral equation for the pairing vertex function $\Phi(\omega_m, k_{\parallel})$ (the one which has a solution at $T = T_c^{\text{ch}}$) is

$$\begin{aligned} & \Phi(\omega_m, k_{\parallel}) \\ &= \frac{\bar{g}_c T}{v_F} \sum_{m'} \int \frac{dk'_{\parallel}}{2\pi} \frac{\Phi(\omega'_m, k'_{\parallel}) \text{sgn}(\omega'_m)}{\omega'_m - i\Sigma(\omega'_m, k'_{\parallel}) - i\mu_B H} \\ & \quad \times \frac{1}{k_{\parallel}^2 + k'_{\parallel}{}^2 - 2\beta k_{\parallel} k'_{\parallel} + \gamma_c |\omega_m - \omega'_m| + \xi_c^{-2}} \\ &= \frac{\bar{g}_c T}{v_F} \sum_{m'} \int \frac{dk'_{\parallel}}{2\pi} \frac{\Phi(\omega'_m, k'_{\parallel}) |\omega'_m - i\Sigma(\omega'_m, k'_{\parallel})|}{[\omega'_m - i\Sigma(\omega'_m, k'_{\parallel})]^2 + (\mu_B H)^2} \\ & \quad \times \frac{1}{k_{\parallel}^2 + k'_{\parallel}{}^2 - 2\beta k_{\parallel} k'_{\parallel} + \gamma_c |\omega_m - \omega'_m| + \xi_c^{-2}}, \end{aligned} \quad (48)$$

where the self-energy is given by Eq. (25).

In the FL regime, when $\lambda_c = \bar{g}_c / (2\pi v_F \xi_c^{-1}) \leq 1$, $\Phi(k_{\parallel}, \omega_m)$ can be, to logarithmical accuracy, approximated by a constant Φ , and Eq. (48) reduces to

$$\Phi = \frac{\lambda_c}{1 + \lambda_c} \log \frac{\omega_{\text{cf}}}{(T_c^2 + H^2)^{1/2}} \Phi. \quad (49)$$

where $\omega_{\text{cf}} \sim \bar{g}_c / \lambda^2$ has been introduced in (27). The superconducting T_c^{ch} becomes zero at a critical λ_c^{cr} , given by

$$\frac{\lambda_c^{\text{cr}}}{1 + \lambda_c^{\text{cr}}} \log \frac{\omega_{\text{cf}}^{\text{cr}}}{H} = 1, \quad (50)$$

or, with logarithmical accuracy, at $\lambda_c^{\text{cr}} \sim 1 / \log(\bar{g}_c / \mu_B H)$. At smaller λ_c , i.e., at larger deviations from CDW QCP, there is no charge-mediated superconductivity.

We solved the gap equation numerically and obtained T_c^{ch} as a function of λ_c and $\mu_B H$. We plot the results in Fig. 11, and present the corresponding phase diagram schematically in Fig. 12. We see that, indeed, superconducting dome gets sharper in the field, i.e., charge-mediated superconductivity gets progressively confined to CDW QCP. We did not do calculations on the other (ordered) side of CDW QCP, but by generic reason we expect a similar shrinking of T_c range. The shrinking of T_c range with increasing field is fully consistent with the experimental data^{33,71}.

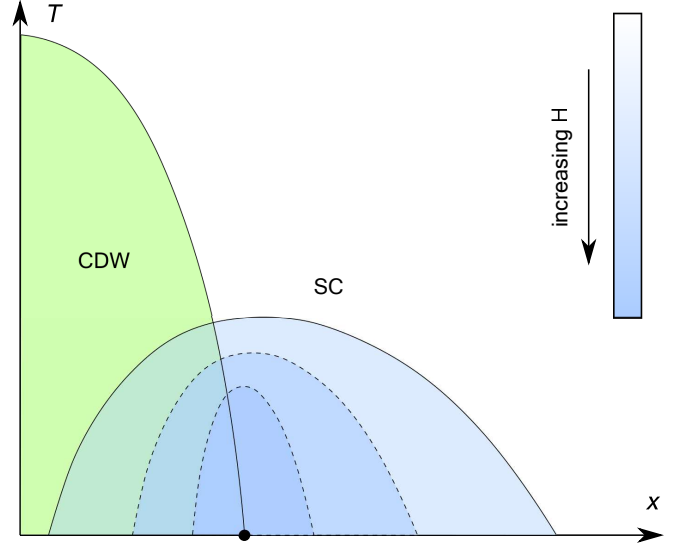


FIG. 12. The variation of the onset temperature of superconducting order mediated by near-critical charge fluctuations in the presence of an external field H . As our numerical results show (Fig. 11), the range of the superconducting dome shrinks as magnetic field increases.

V. CONCLUSION

Motivated by the observation of a static charge order in the cuprates and the enhancement of T_c at its onset, we studied in this work the pairing mediated by charge fluctuations around the quantum-critical point towards an incommensurate charge order with momentum $Q_x = (Q, 0)$ or $Q_y = (0, Q)$. Our main goal was to understand whether charge-mediated pairing near a CDW QCP yields T_c comparable to that obtained from spin-fluctuation exchange.

We first considered a semi-phenomenological charge-fermion model in which hot fermions (the ones at the FS, connected by Q_x or Q_y) interact by exchanging soft collective excitations in the charge channel. We obtained bosonic and fermionic self-energies in the normal state and used them as inputs for the analysis of the quantum-critical pairing problem. We found, in agreement with earlier works⁴⁰ that the charge-mediated pairing interaction is attractive in both d -wave and s -wave channels. The d -wave pairing becomes more favorable once we include other contributions to the pairing interaction from, e.g., antiferromagnetic spin fluctuations. We found that the critical temperature T_c scales with the charge-fermion coupling constant \bar{g}_c , and that fermions from NFL regime very near a hot spot and from a FL region further away from a hot spot contribute to the pairing. In this respect, pairing near a CDW QCP is similar to the pairing by spin fluctuations near a SDW QCP. We obtained the value of $T_c^{\text{ch}} / \bar{g}_c$ numerically.

We next considered the microscopic model in which spin fluctuations emerge at higher energies than charge

fluctuations and are therefore the primary collective degrees of freedom. Charge fluctuations emerge at smaller energies as composite fields, made out of pairs of spin fluctuations. Within this model, we were able to express charge-fermion coupling \bar{g}_c via the underlying spin-fermion coupling \bar{g}_s and relate T_c^{ch} due to charge-fluctuations near a CDW QCP to T_c^{sp} due to spin fluctuations. We found that, at least within RPA, T_c^{ch} due to charge fluctuations is comparable to T_c^{sp} that due to spin fluctuations and may even exceed it, i.e., superconducting T_c does get a substantial enhancement near a CDW QCP.

Finally, we analyzed the behavior of charge-mediated T_c in the presence of a magnetic field and found that the dome of T_c^{ch} around a CDW QCP indeed shrinks as magnetic field increases, because a field destroys superconductivity faster in non-critical regime than in

the quantum-critical regime and hence enhances charge-fluctuation component of T_c near a CDW QCP.

This result and the one that the contribution to T_c from critical charge fluctuations can be larger than the contribution to T_c from non-critical spin-fluctuations, despite that charge fluctuations are by themselves made out of spin fluctuations, may explain the experimental observation that in a magnetic field T_c gets progressively confined to the doping range around the doping at which charge order likely emerges at $T = 0$.

ACKNOWLEDGMENTS

We thank D. Agterberg, E. Berg, R. Fernandes, S. Kivelson, S. Lederer, Y. Shattner, and B. Shklovskii for fruitful discussions. The work was supported by NSF/DMR-1523036.

-
- ¹ J. Tranquada, B. Sternlieb, J. Axe, Y. Nakamura, and S. Uchida, *Nature* **375**, 561 (1995).
 - ² J. Tranquada, J. Axe, N. Ichikawa, A. Moodenbaugh, Y. Nakamura, S. Uchida, *Phys. Rev. Lett.* **78**, 338 (1997).
 - ³ G. Ghiringhelli, M. Le Tacon, M. Minola, S. Blanco-Canosa, C. Mazzoli, N.B. Brookes, G.M. De Luca, A. Frano, D. G. Hawthorn, F. He, T. Loew, M. Moretti Sala, D.C. Peets, M. Salluzzo, E. Schierle, R. Sutarto, G. A. Sawatzky, E. Weschke, B. Keimer, and L. Braicovich, *Science*, **337**, 821 (2012).
 - ⁴ J. Chang, E. Blackburn, A. T. Holmes, N. B. Christensen, J. Larsen, J. Mesot, Ruixing Liang, D. A. Bonn, W. N. Hardy, A. Watenphul, M. v. Zimmermann, E. M. Forgan, and S. M. Hayden, *Nat. Phys.* **8**, 871 (2012).
 - ⁵ A. J. Achkar, R. Sutarto, X. Mao, F. He, A. Frano, S. Blanco-Canosa, M. Le Tacon, G. Ghiringhelli, L. Braicovich, M. Minola, M. Moretti Sala, C. Mazzoli, Ruixing Liang, D. A. Bonn, W. N. Hardy, B. Keimer, G. A. Sawatzky, and D. G. Hawthorn, *Phys. Rev. Lett.*, **109**, 167001 (2012).
 - ⁶ R. Comin, A. Frano, M. M. Yee, Y. Yoshida, H. Eisaki, E. Schierle, E. Weschke, R. Sutarto, F. He, A. Soumyanarayanan, Y. He, M. Le Tacon, I. S. Elfimov, J. E. Hoffman, G. A. Sawatzky, B. Keimer, and A. Damascelli, *Science* **343**, 390 (2014)
 - ⁷ E. H. da Silva Neto, P. Aynajian, A. Frano, R. Comin, E. Schierle, E. Weschke, A. Gyenis, J. Wen, J. Schneeloch, Z. Xu, S. Ono, G. Gu, M. Le Tacon, A. Yazdani, *Science* **343**, 393 (2014).
 - ⁸ K. Fujita, M. H. Hamidian, S. D. Edkins, C. K. Kim, Y. Kohsaka, M. Azuma, M. Takano, H. Takagi, H. Eisaki, S. Uchida, A. Allais, M. J. Lawler, E.-A. Kim, S. Sachdev, and J. C. Séamus Davis, *Proc. Nat. Acad. Sci.* **111**, E3026 (2014).
 - ⁹ Tao Wu, Hadrien Mayaffre, Steffen Krämer, Mladen Horvatić, Claude Berthier, W. N. Hardy, Ruixing Liang, D. A. Bonn, and Marc-Henri Julien, *Nature* **477**, 191-194 (2011); T. Wu, H. Mayaffre, S. Krämer, M. Horvatić, C. Berthier, W.N. Hardy, R. Liang, D.A. Bonn, and M.-H Julien, *Nat. Comm.* **6**, 6438 (2015).
 - ¹⁰ W. Tabis, Y. Li, M. Le Tacon, L Braicovich, A. Kreyssig, M. Minola, G. Dellea, E. Weschke, M. J. Veit, M. Ramazanoglu, A. I. Goldman, T. Schmitt, G. Ghiringhelli, N. Barižic, M. K. Chan, C. J. Dorow, G. Yu, X. Zhao, B. Keimer, and M. Greven, *Nature Communications* **5**, 5875 (2014).
 - ¹¹ M. A. Metlitski and S. Sachdev, *Phys. Rev. B* **82**, 075128 (2010).
 - ¹² K. B. Efetov, H. Meier and C. Pepin, *Nat. Phys.* **9** 442 (2013); H. Meier, M. Eimenkel, C. Pépin, K. B. Efetov, *Phys. Rev. B* **88**, 020506 (2013); H. Meier, C. Pepin, M. Eimenkel and K.B. Efetov, *Phys. Rev. B* **89**, 195115 (2014); K. B. Efetov *Phys. Rev. B* **91**, 045110 (2015).
 - ¹³ S. Sachdev and R. La Placa, *Phys. Rev. Lett.* **111** 027202 (2013); A. Allais, J. Bauer and S. Sachdev, *Phys. Rev. B* **90** 155114 (2014).
 - ¹⁴ Y. Wang and A. V. Chubukov, *Phys. Rev. B* **90** 035149 (2014).
 - ¹⁵ P. A. Lee, *Phys. Rev. X* **4**, 031017 (2014).
 - ¹⁶ C. Pépin, V. S. de Carvalho, T. Kloss, X. Montiel, *Phys. Rev. B* **90**, 195207 (2014); H. Freire, V. S. de Carvalho, and C. Pépin, arXiv:1503.00379 (2015); T. Kloss, X. Montiel, C. Pépin, arXiv:1501.05324 (2015).
 - ¹⁷ D. Chowdhury and S. Sachdev, *Phys. Rev. B* **90**, 134516 (2014).
 - ¹⁸ D. Chowdhury and S. Sachdev, *Phys. Rev. B* **90**, 245136 (2014).
 - ¹⁹ E. Fradkin, S. A. Kivelson, J. M. Tranquada, arXiv:1407.4480.
 - ²⁰ S. Bulut, W. A. Atkinson, and A. P. Kampf, *Phys. Rev. B* **88**, 155132 (2013); W. Atkinson, A. Kampf and S. Bulut, *New J. Phys.* **17** 013025 (2015); W. A. Atkinson and A. P. Kampf, *Phys. Rev. B* **91**, 104509 (2015).
 - ²¹ Y. Wang and A.V. Chubukov, *Phys. Rev. B* **91**, 195113 (2015).
 - ²² J. Xia, E. Schemm, G. Deutscher, S. A. Kivelson, D. A. Bonn, W. N. Hardy, R. Liang, W. Siemons, G. Koster, M. M. Fejer, and A. Kapitulnik *Phys. Rev. Lett.* **100**, 127002 (2008); H. Karapetyan, J. Xia, M. Hucker, G. D. Gu, J. M. Tranquada, M. M. Fejer, and A. Kapitulnik, *Phys. Rev.*

- Lett. **112**, 047003 (2014). See also Y. Lubashevsky, LiDong Pan, T. Kirzhner, G. Koren, and N. P. Armitage, Phys. Rev. Lett. **112**, 147001, (2014).
- ²³ Y. Sidis and P. Bourges, arXiv: 1306.5124 (2013); L. Mangin-Thro, Y. Sidis, A. Wildes, P. Bourges, arXiv: 1501.04919 (2015).
- ²⁴ L. Nie, G. Tarjus, and S. A. Kivelson, Proc. Nat. Acad. Sci. **111**, 7980 (2014).
- ²⁵ A. Tsvelik and A. V. Chubukov, Phys. Rev. B **89**, 184515 (2014).
- ²⁶ D.F. Agterberg, D.S. Melchert, and M.K. Kashyap, Phys. Rev. B **91**, 054502 (2015).
- ²⁷ S. Bulut, Arno P. Kampf, W. A. Atkinson, arXiv:1503.08896.
- ²⁸ O. Cyr-Choinière, G. Grissonnanche, S. Badoux, J. Day, D. A. Bonn, W. N. Hardy, R. Liang, N. Doiron-Leyraud, L. Taillefer, arXiv:1504.06972.
- ²⁹ see N Harrison and S E Sebastian, New J. Phys. **16**, 063025 (2014) and references therein.
- ³⁰ A. R. Moodenbaugh, Youwen Xu, M. Suenaga, T. J. Folkerts, and R. N. Shelton, Phys. Rev. B **38**, 4596 (1988)
- ³¹ Ruixing Liang, D. A. Bonn, and W. N. Hardy, Phys. Rev. B **73**, 180505(R) (2006).
- ³² O. Cyr-Choinière, D. LeBoeuf, S. Badoux, S. Dufour-Beauséjour, D. A. Bonn, W. N. Hardy, R. Liang, N. Doiron-Leyraud, L. Taillefer, arXiv:1503.02033.
- ³³ G. Grissonnanche *et al.*, Nat. Comm. **5**, 3280 (2014).
- ³⁴ S. Sachdev and B. Keimer, Physics Today, **64**, 29 (2011).
- ³⁵ L. Benfatto, M. Capone, S. Caprara, C. Castellani, and C. Di Castro, Phys. Rev. B **78**, 140502(R) (2008).
- ³⁶ A. Chubukov, D. Pines and J. Schmalian *A Spin Fluctuation Model for D-wave Superconductivity* in ‘The Physics of Conventional and Unconventional Superconductors’ edited by K.H. Bennemann and J.B. Ketterson (Springer-Verlag), 2002; P. Monthoux, D. Pines, and G. G. Lonzarich, Nature **450**, 1177-1183 (2007); D. J. Scalapino, Rev. Mod. Phys. **84**, 1383 (2012). For the latest development see T.A. Maier, P. Staar, and D.J. Scalapino, submitted.
- ³⁷ H. v. Löhneysen, A. Rosch, M. Vojta, and P. Wölfle, Rev. Mod. Phys. **79**, 1015 (2007).
- ³⁸ E. Fradkin, S. A. Kivelson, M. J. Lawler, J. P. Eisenstein, A. P. Mackenzie, Annual Reviews of Condensed Matter Physics **1**, 153 (2010).
- ³⁹ D. Bergeron, D. Chowdhury, M. Punk, S. Sachdev, and A.-M. S. Tremblay, Phys. Rev. B **86**, 155123 (2012)
- ⁴⁰ C. Castellani, C. Di Castro, and M. Grilli, Phys. Rev. Lett. **75**, 4650 (1995); A. Perali, C. Castellani, C. Di Castro, and M. Grilli, Phys. Rev. B **54**, 16216 (1996); C. Castellani *et al.*, J. Phys. Chem. Sol. **59**, 1694 (1998); A. Perali *et al.*, Phys. Rev. B **62**, R9295(R) (2000); S. Andergassen, S. Caprara, C. Di Castro, and M. Grilli, Phys. Rev. Lett. **87**, 056401 (2001); G. Seibold *et al.*, Physica C **481**, 132 (2012).
- ⁴¹ K. Le Hur and T. M. Rice, Ann. Phys. **324**, 1452 (2009).
- ⁴² A. Greco and M. Bejas, Phys. Rev. B **83**, 212503 (2011).
- ⁴³ V. Mishra and M. R. Norman, arXiv:1502.02782; M. R. Norman, Phys Rev B **91**, 140505(R) (2015).
- ⁴⁴ Y. Wang, D. Agterberg, and A. V. Chubukov, Phys. Rev. B **91**, 115103 (2015); Phys. Rev. Lett. **114**, 197001 (2015).
- ⁴⁵ A. Georges, G. Kotliar, W. Krauth, and M. J. Rozenberg Rev. Mod. Phys. **68**, 13 (1996); P. A. Lee, N. Nagaosa, and X-G Wen, Rev. Mod. Phys. **78**, 17 (2006); D. B. Kyung, S. S. Kancharla, D. Sénéchal, A.-M. S. Tremblay, M. Civelli, and G. Kotliar, Phys. Rev. B **73**, 165114 (2006); E. Gull, O. Parcollet, and A. J. Millis, Phys. Rev. Lett. **110**, 216405 (2013); G. Sordi, P. Sémon, K. Haule, and A.-M. S. Tremblay Phys. Rev. B **87**, 041101(R) (2013); Ara Go and A. J. Millis, Phys. Rev. Lett. **114**, 016402 (2015) and references therein
- ⁴⁶ Y. Wang and A. V. Chubukov, Phys. Rev. Lett. **110**, 127001 (2013).
- ⁴⁷ M. Metlitski, D. Mross, S. Sachdev, and T. Senthil, Phys. Rev. B **91**, 115111 (2015).
- ⁴⁸ D. F. Mross, J. McGreevy, H. Liu, and T. Senthil, Phys. Rev. B **82**, 045121 (2010).
- ⁴⁹ S. Lederer, Y. Schattner, E. Berg, and S. A. Kivelson, Phys. Rev. Lett. **114**, 097001 (2015).
- ⁵⁰ S.-S. Lee, Phys. Rev. B **80**, 165102 (2009).
- ⁵¹ P. A. Lee, Phys. Rev. Lett. **63**, 680 (1989); J. Polchinski, Nucl. Phys. B **422**, 617 (1994); Y.-B. Kim, A. Furusaki, X.-G. Wen, and P. A. Lee, Phys. Rev. B **50**, 17917 (1994); C. Nayak and F. Wilczek, Nucl. Phys. B **417**, 359 (1994); **430**, 534 (1994); B. L. Altshuler, L. B. Ioffe, and A. J. Millis, Phys. Rev. B **50**, 14048 (1994); **52**, 5563 (1995); S. Chakravarty, R. E. Norton, and O. F. Syjuasen, Phys. Rev. Lett. **74**, 1423 (1995); C.J. Halboth and W. Metzner, Phys. Rev. Lett. **85**, 5162 (2000); J. Quintanilla and A. J. Schofield, Phys. Rev. B **74**, 115126 (2006); J. Rech, C. Pépin, and A. V. Chubukov, Phys. Rev. B **74**, 195126 (2006); T. Senthil, Phys. Rev. B **78**, 035103 (2008); M. Zacharias, P. Wölfle, and M. Garst, Phys. Rev. B **80**, 165116 (2009); D.L. Maslov and A.V. Chubukov, Phys. Rev. B **81**, 045110 (2010). M.A. Metlitski and S. Sachdev, Phys. Rev. B **82**, 075127 (2010); D. F. Mross, J. McGreevy, H. Liu, and T. Senthil, Phys. Rev. B **82**, 045121 (2010).
- ⁵² Ar. Abanov, A. V. Chubukov, and J. Schmalian, Adv. Phys. **52**, 119 (2003).
- ⁵³ A. Liam Fitzpatrick, Shamit Kachru, Jared Kaplan, S. Raghu, Gonzalo Torroba, Huajia Wang, arXiv:1410.6814; A. V. Chubukov and J. Schmalian, Phys. Rev. B **72**, 174520 (2005); E-G Moon and A. V. Chubukov, JLTP, **161**, 263 (2010); Ar. Abanov *et al.*, to appear.
- ⁵⁴ R. Comin, R. Sutarto, E. H. da Silva Neto, L. Chauviere, R. Liang, W. N. Hardy, D. A. Bonn, F. He, G. A. Sawatzky, A. Damascelli, Science, **347** 1335 (2015).
- ⁵⁵ D. Bergeron, D. Chowdhury, M. Punk, S. Sachdev, and A.-M. S. Tremblay, Phys. Rev. B **86**, 155123 (2012).
- ⁵⁶ S. A. Hartnoll, D. M. Hofman, M. A. Metlitski, and S. Sachdev, Phys. Rev. B **84**, 125115 (2011).
- ⁵⁷ M. Zacharias, P. Wölfle, and M. Garst, Phys. Rev. B **80**, 165116 (2009).
- ⁵⁸ D. T. Son, Phys. Rev. D. **59**, 094019 (1999).
- ⁵⁹ A. Chubukov and J. Schmalian, Phys. Rev. B. **72**, 174520 (2005).
- ⁶⁰ A. L. Fitzpatrick, S. Kachru, J. Kaplan, S. Raghu, G. Torroba, and H. Wang, arXiv:1410.6814.
- ⁶¹ R. Nandkishore, L. Levitov, and A. V. Chubukov, Nat. Phys. **8**, 158 (2012).
- ⁶² Ar. Abanov, A. V. Chubukov, and A.M. Finkelstein, Europhys. Lett. **54**, 488 (2001)
- ⁶³ M. R. Norman, Phys. Rev. B **75**, 184514 (2007).
- ⁶⁴ W. L. McMillan, Phys. Rev. **167**, 331 (1968).
- ⁶⁵ Ar. Abanov, A. V. Chubukov, and M. R. Norman, Phys. Rev. B **78**, 220507(R) (2008).
- ⁶⁶ R. Haslinger and A. V. Chubukov, Phys. Rev. B **68**, 214508 (2003); R. Haslinger and A. V. Chubukov, Phys. Rev. B **67**, 140504(R) (2003).
- ⁶⁷ E. Berg, M. A. Metlitski, and S. Sachdev Science **338**, 1606 (2012).

- ⁶⁸ A. V. Chubukov and P. Wölfle Phys. Rev. B **89**, 045108 (2014).
- ⁶⁹ S. Maiti and A. V. Chubukov in “Proceedings of the XVII Training Course in the physics of Strongly Correlated Systems”, Vietri sul Mare (Salerno), Italy (2013); “Novel Superfluids”, Chapter 15, Oxford Press, (2014).
- ⁷⁰ A. V. Chubukov, D. L. Maslov, and V. I. Yudson Phys. Rev. B **89**, 155126 (2014).
- ⁷¹ B. J. Ramshaw, S. E. Sebastian, R. D. McDonald, James Day, B. S. Tan, Z. Zhu, J.B. Betts, R. Liang, D. A. Bonn, W. N. Hardy, and N. Harrison, Science **348**, 317 (2015).